

Neutral Organic Mixed-Valence Compounds: Synthesis and All-Optical Evaluation of Electron-Transfer Parameters

Alexander Heckmann and Christoph Lambert*

Contribution from the Institut für Organische Chemie, Universität Würzburg, Am Hubland, D-97074 Würzburg, Germany

Received November 17, 2006; E-mail: lambert@chemie.uni-wuerzburg.de

Abstract: In this paper we present the synthesis as well as a detailed study of the electrochemical and photophysical properties of a series of neutral organic mixed-valence (MV) compounds, **1–7**, in which different amine donor centers are connected to perchlorinated triarylmethyl radical units by various spacers. We show that this new class of compounds are excellent model systems for the investigation of electron transfer due to their uncharged character and, consequently, their excellent solubility, particularly in nonpolar solvents. A detailed band shape analysis of the intervalence charge-transfer (IV-CT) bands in the context of Jortner's theory allowed the electron-transfer parameters (inner vibrational reorganization energy λ_v , outer solvent reorganization energy λ_o , and the difference in the free energy between the diabatic ground and excited states, ΔG° , as well as the averaged molecular vibrational mode $\bar{\nu}_v$) to be extracted independently. In this way we were able to analyze the solvatochromic behavior of the IV-CT bands by evaluating the contribution of each parameter. By comparison of different compounds, we were also able to assign specific molecular moieties to changes in $\bar{\nu}_v$. For this class of molecules, we also demonstrate that the adiabatic dipole moment difference $\Delta\mu_{ab}$ and, consequently, the electronic coupling V_{12} can be evaluated directly from the absorption spectra by a new variant of the solvatochromic method. Furthermore, an investigation of the electrochemistry of compounds **1–7** by cyclic voltammetry as well as spectroelectrochemistry shows that, not only in the neutral MV compounds but also in their oxidized forms, a charge transfer can be optically induced but with exchanged donor–acceptor functionalities of the redox centers.

Introduction

Organic mixed-valence (MV) compounds are the focus of recent research because they are simple and suitable model systems for the investigation of electron-transfer (ET) processes.^{1–5} Usually these MV systems consist of two redox centers in different redox states, linked by a saturated or unsaturated bridge unit. Many investigations have focused on the influence of the type and the length of the bridge unit (spacer)^{6–25} or the nature of the redox centers on the electronic coupling V_{12} . This coupling

is a measure of the electronic communication between two states in which the charge is located at either redox center. In this respect also multidimensional MV compounds^{16,26–31} (with three or more redox centers) as well as symmetrical^{10–14,17,23–25,29,32–42}

- (1) Brunschwig, B. S.; Creutz, C.; Sutin, N. *Chem. Soc. Rev.* **2002**, *31*, 168–184.
- (2) Launay, J.-P. *Chem. Soc. Rev.* **2001**, *30*, 386–397.
- (3) Chen, P.; Meyer, T. J. *Chem. Rev.* **1998**, *98*, 1439–1478.
- (4) Nelsen, S. F.; Ismagilov, R. F.; Trieber, D. A. *Science* **1997**, *278*, 846–849.
- (5) Balzani, V., Ed. *Electron Transfer in Chemistry, Vols. 1–5*; Wiley-VCH: Weinheim, 2001.
- (6) Nelsen, S. F.; Li, G.; Konradsson, A. *Org. Lett.* **2001**, *3*, 1583–1586.
- (7) Lambert, C.; Nöll, G.; Schelter, J. *Nat. Mater.* **2002**, *1*, 69–73.
- (8) Lambert, C.; Nöll, G. *J. Am. Chem. Soc.* **1999**, *121*, 8434–8442.
- (9) Rosokha, S. V.; Sun, D.-L.; Kochi, J. K. *J. Phys. Chem. A* **2002**, *106*, 2283–2292.
- (10) Mayor, M.; Büschel, M.; Fromm, K. M.; Lehn, J.-M.; Daub, J. *Chem. Eur. J.* **2001**, *7*, 1266–1272.
- (11) Barlow, S.; Risko, C.; Chung, S.-J.; Tucker, N. M.; Coropceanu, V.; Jones, S. C.; Levi, Z.; Brédas, J. L.; Marder, S. R. *J. Am. Chem. Soc.* **2005**, *127*, 16900–16911.
- (12) Heckmann, A.; Amthor, S.; Lambert, C. *Chem. Commun.* **2006**, *28*, 2959–2961.
- (13) Amthor, S.; Lambert, C. *J. Phys. Chem. A* **2006**, *110*, 1177–1189.
- (14) Lindeman, S. V.; Rosokha, S. V.; Sun, D.; Kochi, J. K. *J. Am. Chem. Soc.* **2002**, *124*, 843–855.
- (15) Nelsen, S. F.; Tran, H. Q. *J. Phys. Chem. A* **1999**, *103*, 8139–8144.
- (16) Lambert, C.; Nöll, G. *Chem. Eur. J.* **2002**, *8*, 3467–3477.
- (17) Coropceanu, V.; Malagoli, M.; André, J. M.; Brédas, J. L. *J. Am. Chem. Soc.* **2002**, *124*, 10519–10530.
- (18) Lambert, C.; Amthor, S.; Schelter, J. *J. Phys. Chem. A* **2004**, *108*, 6474–6486.
- (19) Lambert, C.; Risko, C.; Coropceanu, V.; Schelter, J.; Amthor, S.; Gruhn, N. E.; Durivage, J. C.; Brédas, J. L. *J. Am. Chem. Soc.* **2005**, *127*, 8508–8516.
- (20) Nelsen, S. F.; Tran, H. Q.; Nagy, M. A. *J. Am. Chem. Soc.* **1998**, *120*, 298–304.
- (21) Nelsen, S. F.; Ismagilov, R. F.; Powell, D. R. *J. Am. Chem. Soc.* **1998**, *120*, 1924–1925.
- (22) Barlow, S.; Risko, C.; Coropceanu, V.; Tucker, N. M.; Jones, S. C.; Levi, Z.; Khrustalev, V. N.; Antipin, M. Y.; Kinnibrugh, T. L.; Timofeeva, T.; Marder, S. R.; Brédas, J. L. *Chem. Commun.* **2005**, 764–766.
- (23) Holzapfel, M.; Lambert, C.; Selinka, C.; Stalke, D. *J. Chem. Soc., Perkin Trans. 2* **2002**, 1553–1561.
- (24) Bonvoisin, J.; Launay, J.-P.; Rovira, C.; Veciana, J. *Angew. Chem., Int. Ed.* **1994**, *33*, 2106–2109.
- (25) Rovira, C.; Ruiz-Molina, D.; Elsner, O.; Vidal-Gancedo, J.; Bonvoisin, J.; Launay, J.-P.; Veciana, J. *Chem. Eur. J.* **2001**, *7*, 240–250.
- (26) Bonvoisin, J.; Launay, J.-P.; Verbouwe, W.; Van, der Auweraer, M.; De, Schryver, F. C. *J. Phys. Chem.* **1996**, *100*, 17079–17082.
- (27) Lambert, C.; Nöll, G. *Angew. Chem., Int. Ed.* **1998**, *37*, 2107–2110.
- (28) Lambert, C.; Nöll, G.; Hampel, F. *J. Phys. Chem. A* **2001**, *105*, 7751–7758.
- (29) Sedo, J.; Ruiz, D.; Vidal-Gancedo, J.; Rovira, C.; Bonvoisin, J.; Launay, J.-P.; Veciana, J. *Synth. Met.* **1997**, *85*, 1651–1654.
- (30) Stickle, K. R.; Blackstock, S. C. *Tetrahedron Lett.* **1995**, *36*, 1585–1588.
- (31) Lambert, C.; Nöll, G.; Schmälzlin, E.; Meerholz, K.; Bräuchle, C. *Chem. Eur. J.* **1998**, *4*, 2129–2135.
- (32) Risko, C.; Barlow, S.; Coropceanu, V.; Halik, M.; Brédas, J. L.; Marder, S. R. *Chem. Commun.* **2003**, 194–195.

(with two degenerate redox centers) and asymmetrical^{43–45} MV species (with two non-degenerate redox centers) have been investigated. The influence of temperature¹⁵ and solvent polarity^{46,47} on electron transfer in organic MV compounds was also studied. All the above-mentioned MV compounds are either radical cations or radical anions. However, quite recently, Veciana et al. synthesized organic–inorganic hybrid MV compounds consisting of an organic perchlorinated triarylmethyl radical acceptor and a ferrocene donor center.^{48–50}

While the evaluation of ET parameters in MV compounds is of prime interest, the determination of these parameters often involves major inaccuracies and, in particular, possibly erroneous assumptions about the effective ET distance. In this paper we outline a procedure that yields reliable ET parameters within the given framework of the applied theoretical model. These parameters were evaluated using a specifically designed set of suitable MV compounds as described below.

The adiabatic potential energy surfaces (PES) of the ground state and the excited state of a MV system with two redox states can be calculated in the context of a two-state model by solving secular eq 1, where harmonic potentials are used for the diabatic (non-interacting) states along an ET coordinate x (Figure 1).^{51–54} In MV compounds the optically induced ET from the ground state to the excited state is associated with a so-called intervalence charge-transfer (IV-CT) band in the near-infrared (Figure 1). Within the framework of generalized Mulliken–Hush (GMH) theory,^{54–57} the parameters describing the ET can be evaluated by analyzing the IV-CT band (eqs 2–4).^{58–63} In this

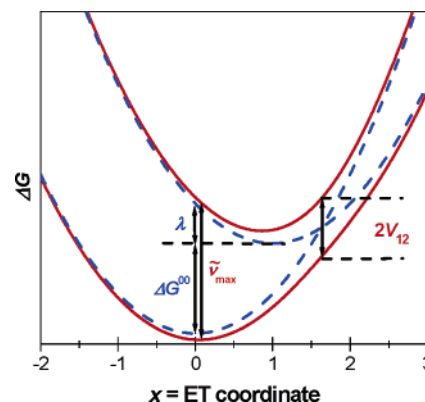


Figure 1. Diabatic (dashed blue) and adiabatic (solid red) potential energy surfaces (PES) of a one-dimensional MV system with two non-degenerate redox centers. V_{12} is the coupling energy, λ the Marcus reorganization energy, and ΔG° the difference in the free energy between the diabatic states. In the weak coupling regime ($V_{12} \rightarrow 0$), $\tilde{\nu}_{\max}$ corresponds to the sum of λ and ΔG° .

context, in the weak coupling regime ($V_{12} \rightarrow 0$),^{3,52} the maximum of the IV-CT band $\tilde{\nu}_{\max}$ corresponds to the sum of the Marcus reorganization energy λ and the difference between the free energies of the minima of the diabatic states ΔG° (Figure 1). We point out here that the PES in Figure 1 does apply for the situation of the MV systems outlined below. In these cases, ΔG° is in fact so strong compared to the reorganization energy that no double minimum potential is present in the ground-state adiabatic potential curve.

The reorganization energy λ can be partitioned into two terms (eq 5): the outer solvent reorganization energy λ_o , which characterizes the energy needed for the reorientation of the solvent after ET has taken place, and the inner vibrational reorganization energy λ_v , describing the energy corresponding to geometrical changes of the molecule during ET. However, it is difficult to obtain the values for ΔG° , λ_o , and λ_v separately by a Marcus–Hush analysis.^{58–63}

$$\begin{vmatrix} V_{11} - E & V_{12} \\ V_{12} & V_{22} - E \end{vmatrix} = 0 \quad (1)$$

$$\text{with } V_{11} = \lambda x^2 \quad \text{and} \quad V_{22} = \lambda(1-x)^2 + \Delta G^{\circ}$$

$$V_{12} = \frac{\mu_{ab} \tilde{\nu}_{\max}}{\Delta\mu_{12}} \quad \text{with} \quad \tilde{\nu}_{\max} = \Delta G^{\circ} + \lambda \quad (2)$$

$$\mu_{ab} = \sqrt{\frac{3hc\epsilon_0 \ln 10}{2000 \pi^2 N} \frac{9n}{(n^2 + 2)^2} \int \frac{\epsilon}{\tilde{\nu}} d\tilde{\nu}} \quad (3)$$

$$\Delta\mu_{12} = \sqrt{\Delta\mu_{ab}^2 + 4\mu_{ab}^2} \quad (4)$$

where E is the eigenvector, λ the Marcus reorganization energy,

$$\lambda = \lambda_o + \lambda_v \quad (5)$$

x the ET coordinate, ΔG° the free energy difference between the adiabatic ground and excited states, μ_{ab} the transition moment between the adiabatic states, $\tilde{\nu}_{\max}$ the absorption maximum of the IV-CT band, $\Delta\mu_{12}$ the diabatic dipole moment difference, h Planck's constant, c the speed of light, ϵ_0 the permittivity of

- (33) Nelsen, S. F.; Weaver, M. N.; Zink, J. I.; Telo, J. P. *J. Am. Chem. Soc.* **2005**, *127*, 10611–10622.
 (34) Nelsen, S. F.; Konradsson, A. E.; Weaver, M. N.; Telo, J. P. *J. Am. Chem. Soc.* **2003**, *125*, 12493–12501.
 (35) Bailey, S.; Zink, J. I.; Nelsen, S. F. *J. Am. Chem. Soc.* **2003**, *125*, 5939–5947.
 (36) Coropceanu, V.; Malagoli, M.; Andre, J. M.; Brédas, J. L. *J. Chem. Phys.* **2001**, *115*, 10409–10416.
 (37) Low, P. J.; Paterson, M. A. J.; Puschmann, H.; Goeta, A. E.; Howard, J. A. K.; Lambert, C.; Cherryman, J. C.; Tackley, D. R.; Leeming, S.; Brown, B. *Chem. Eur. J.* **2004**, *10*, 83–91.
 (38) Nelsen, S. F.; Chang, H.; Wolff, J. J.; Adamus, J. *J. Am. Chem. Soc.* **1993**, *115*, 12276–12289.
 (39) Nelsen, S. F.; Ismagilov, R. F.; Gentile, K. E.; Powell, D. R. *J. Am. Chem. Soc.* **1999**, *121*, 7108–7114.
 (40) Nelsen, S. F.; Ismagilov, R. F.; Teki, Y. *J. Am. Chem. Soc.* **1998**, *120*, 2200–2201.
 (41) Lahlil, K.; Moradpour, A.; Bowlas, C.; Menou, F.; Cassoux, P.; Bonvoisin, J.; Launay, J.-P.; Dive, G.; Dehareng, D. *J. Am. Chem. Soc.* **1995**, *117*, 9995–10002.
 (42) Elsner, O.; Ruiz-Molina, D.; Vidal-Gancedo, J.; Rovira, C.; Veciana, J. *Nano Lett.* **2001**, *1*, 117–120.
 (43) Yano, M.; Ishida, Y.; Aoyama, K.; Tatsumi, M.; Sato, K.; Shiomi, D.; Ichimura, A.; Takui, T. *Synth. Met.* **2003**, *137*, 1275–1276.
 (44) Lambert, C.; Nöll, G. *J. Chem. Soc., Perkin Trans. 2* **2002**, 2039–2043.
 (45) Nelsen, S. F. *Chem. Eur. J.* **2000**, *6*, 581–588.
 (46) Nelsen, S. F.; Trieber, D. A.; Ismagilov, R. F.; Teki, Y. *J. Am. Chem. Soc.* **2001**, *123*, 5684–5694.
 (47) Nelsen, S. F.; Ismagilov, R. F. *J. Phys. Chem. A* **1999**, *103*, 5373–5378.
 (48) Elsner, O.; Ruiz-Molina, D.; Ratera, I.; Vidal-Gancedo, J.; Rovira, C.; Veciana, J. *J. Organomet. Chem.* **2001**, *637–639*, 251–257.
 (49) Sporer, C.; Ratera, I.; Ruiz-Molina, D.; Zhao, Y.; Vidal-Gancedo, J.; Wurst, K.; Jaitner, P.; Clays, K.; Persoons, A.; Rovira, C.; Veciana, J. *Angew. Chem., Int. Ed.* **2004**, *43*, 5266–5268.
 (50) Ratera, I.; Ruiz-Molina, D.; Renz, F.; Enslin, J.; Wurst, K.; Rovira, C.; Gütllich, P.; Veciana, J. *J. Am. Chem. Soc.* **2003**, *125*, 1462–1463.
 (51) Sutin, N. *Prog. Inorg. Chem.* **1983**, *30*, 441–498.
 (52) Brunschwig, B. S.; Sutin, N. *Coord. Chem. Rev.* **1999**, *187*, 233–254.
 (53) Creutz, C. *Prog. Inorg. Chem.* **1983**, *30*, 1–73.
 (54) Creutz, C.; Newton, M. D.; Sutin, N. *J. Photochem. Photobiol. A: Chem.* **1994**, *82*, 47–59.
 (55) Cave, R. J.; Newton, M. D. *Chem. Phys. Lett.* **1996**, *249*, 15–19.
 (56) Cave, R. J.; Newton, M. D. *J. Chem. Phys.* **1997**, *106*, 9213–9226.
 (57) Newton, M. D. *Adv. Chem. Phys.* **1999**, *106*, 303–375.
 (58) Hush, N. S. *Coord. Chem. Rev.* **1985**, *64*, 135–157.
 (59) Hush, N. S. *Electrochim. Acta* **1968**, *13*, 1005–1023.
 (60) Reimers, J. R.; Hush, N. S. *Chem. Phys.* **1989**, *134*, 323–354.
 (61) Hush, N. S. *Chem. Phys.* **1975**, *11*, 361–366.
 (62) Cave, R. J.; Newton, M. D. *Chem. Phys. Lett.* **1996**, *249*, 15–19.

- (63) Newton, M. D.; Cave, R. J. In *Molecular Electronics*; Jortner, J., Ratner, M. A., Eds.; Blackwell Science: Oxford, UK, 1997; p 73.

the vacuum, N Avogadro's number, n the refractive index of solvent, ϵ the extinction coefficient, $\Delta\mu_{ab}$ the adiabatic dipole moment difference, λ_o the outer solvent reorganization energy, and λ_v the inner vibrational reorganization energy.

Because both the solvent reorganization energy λ_o and $\Delta G^{\circ\circ}$ depend on the polarity of the solvent, IV-CT bands are expected to show a solvatochromic behavior. However, because of the charged character of organic MV compounds, their solubility, especially in nonpolar solvents, usually is not high enough to allow the study of the solvent dependence of IV-CT bands in a broader range of solvents.⁴⁶ While the transition moment μ_{ab} of the IV-CT band can be determined easily with eq 3 by integration of the reduced absorption band,⁶⁴ it is much more complicated to obtain a reliable value for the diabatic dipole moment difference between the two diabatic states $\Delta\mu_{12}$, which is needed for the evaluation of the electronic coupling V_{12} via eq 2. However, the diabatic dipole moment difference $\Delta\mu_{12}$ can be calculated by eq 4 from the difference of the adiabatic dipole moments $\Delta\mu_{ab}$ and the transition moment μ_{ab} . Unfortunately, $\Delta\mu_{ab}$ cannot be obtained directly by a Hush analysis of the IV-CT band but must be either estimated from the geometrical distance between the two redox centers or calculated by quantum chemical methods. Both methods are afflicted with major inaccuracies,⁶⁵ and the experimental determination of $\Delta\mu_{ab}$ by means of electro-optical absorption measurements (EOAM)^{66–70} unfortunately is very complicated for charged species because of ion migration in the electric field.

All the above-mentioned disadvantages can be circumvented by using neutral MV systems, a class of organic molecules which has, to our knowledge, never been investigated in detail before our quite recent communication on the synthesis of the first neutral organic MV compound **1**.^{71,72} The neutral character of **1** facilitated the acquisition of ultraviolet/visible/near-infrared (UV/vis/NIR) spectra in a broad variety of solvents, ranging from totally nonpolar (*n*-hexane) to strongly polar (acetonitrile), and allowed us to accomplish a band-shape analysis of the IV-CT band of this MV compound with the aid of a golden rule expression (eq 6)⁷³ in the context of Jortner's theory.^{74–76}

$$\epsilon/\tilde{\nu} = \frac{2000 N\pi^2 (n^2 + 2)^2}{3\epsilon_o \ln 10} \frac{1}{9n} \mu_{ab}^2 \sum_{j=0}^{\infty} \frac{e^{-S} S^j}{j!} \sqrt{\frac{1}{4\pi hc \lambda_o kT}} \times \exp\left[-\frac{hc(j\tilde{\nu}_v + \lambda_o - \tilde{\nu} + \Delta G^{\circ\circ})^2}{4\lambda_o kT}\right] \quad (6)$$

with Huang–Rhys factor $S = (\lambda_v/\tilde{\nu}_v)$

This model, which can be applied to the analysis of both fluorescence emission^{76,77} and absorption spectra,^{74,77,78} is based on a semiclassical approach that considers a classical solvent mode and a single high-temperature averaged molecular vibration mode $\tilde{\nu}_v$, which is treated quantum chemically.³ Thereby, the values for $\Delta G^{\circ\circ}$, $\tilde{\nu}_v$, and the reorganization energies λ_o and λ_v can be extracted separately from the absorption spectrum by a least-squares fit of the IV-CT band varying these four parameters in eq 6. However, while a Hush analysis is only accurately applicable for nearly Gaussian-shaped bands, a Jortner fit is generally limited to unsymmetrical bands, since otherwise the parameters are dependent and too ambiguous. The main factors that determine the asymmetry of the IV-CT bands are the averaged molecular vibration mode $\tilde{\nu}_v$ and the inner reorganization energy λ_v . The ratio $S = \lambda_v/\tilde{\nu}_v$ (Huang–Rhys factor) is a measure of the electron–phonon coupling, i.e., the number of vibrations generated during the vertical electronic transition. Large factors produce Gaussian-shaped bands, while small factors lead to asymmetric absorption bands.⁷⁹ Thus, only systems with small Huang–Rhys factors may be analyzed with Jortner's theory accurately.

In the following we present the synthesis and electrochemical properties of a series of neutral MV compounds, **1–7**, where perchlorinated triarylmethyl (PCTM) radical centers are linked by various spacers to nitrogen donor centers. Furthermore, owing to the neutral character of these MV compounds, we were able to perform a detailed investigation of the solvatochromic behavior of these compounds in the context of Jortner's theory which will yield insight into the parameters governing the ET behavior in **1–7**. In addition, we investigated the solvatochromic behavior of these ET parameters in order to obtain reliable values for the diabatic dipole moment differences $\Delta\mu_{12}$. The latter will allow us to calculate accurately the electronic coupling V_{12} by eq 4 of all compounds **1–7**.

Results and Discussion

Synthesis. The last step of the syntheses of all PCTM radicals is the *in situ* generation of the corresponding carbanions starting from the α -H compounds and their oxidation to the radicals with *p*-chloranil in dimethylsulfoxide (DMSO). The synthesis of radical **1** was described previously.⁷¹ In order to synthesize a great number of differently substituted triarylmethyl radicals, the perchlorinated compound **8** is a useful intermediate (Scheme 1). With this compound **8**, we were able to synthesize the donor-substituted triarylmethyl radicals **2**, **5**, **6**, and **7** with an alkynyl spacer via Stille coupling, compound **4** with a biphenyl spacer by a Suzuki coupling, and radical **3** via a Buchwald–Hartwig

(64) Birks, J. B., Ed. *Photophysics of Aromatic Molecules*; Wiley-Interscience: New York, 1969; Chapter 3.5–3.7.

(65) While *ab initio* and semiempirical UHF methods tend to overemphasize charge localization, DFT calculations usually overemphasize charge delocalization; see ref 11 in Lent, C. S.; Isaksen, B.; Liebermann, M. *J. Am. Chem. Soc.* **2003**, *125*, 1056. Nelsen et al. recently demonstrated that the often used N–N distance in bis(triarylamine) radical cations results in too large effective ET distances; see ref 34.

(66) Wortmann, R.; Krämer, P.; Glania, C.; Lebus, S.; Detzer, N. *Chem. Phys.* **1993**, *173*, 99–108.

(67) Oh, D. H.; Sano, M.; Boxer, S. G. *J. Am. Chem. Soc.* **1991**, *113*, 6880–6890.

(68) Brunschwig, B. S.; Creutz, C.; Sutin, N. *Coord. Chem. Rev.* **1998**, *177*, 61–79.

(69) Treynor, T. P.; Boxer, S. G. *J. Phys. Chem. A* **2004**, *108*, 1764–1778.

(70) Coe, B. J.; Harris, J. A.; Jones, L. A.; Brunschwig, B. S.; Song, K.; Clays, K.; Garin, J.; Orduna, J.; Coles, S. J.; Hursthouse, M. B. *J. Am. Chem. Soc.* **2005**, *127*, 4845–4859.

(71) Heckmann, A.; Lambert, C.; Goebel, M.; Wortmann, R. *Angew. Chem., Int. Ed.* **2004**, *43*, 5851–5856.

(72) See footnote 19 in ref 71.

(73) We derived eq 6 from eq 4a given in ref 74, where we replaced $V^2\Delta\mu^2$ by $(M_e h\nu)^2$ (given in their notation). Thus, in contrast to ref 74, we assume a frequency-independent transition moment M_e , which is an observable, rather than a frequency-independent product $V^2\Delta\mu^2$, which consists of diabatic (not observable) quantities. See also: Marcus, R. A. *J. Phys. Chem.* **1989**, *93*, 3078–3086.

(74) Gould, I. R.; Noukakis, D.; Gomez-Jahn, L.; Young, R. H.; Goodman, J. L.; Farid, S. *Chem. Phys.* **1993**, *176*, 439–456.

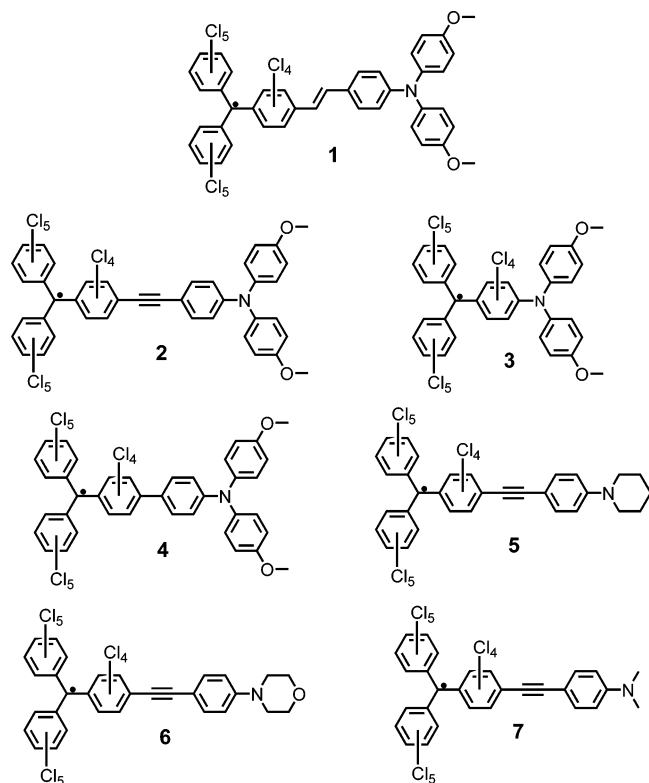
(75) Nelsen, S. F.; Ramm, M. T.; Wolff, J. J.; Powell, D. R. *J. Am. Chem. Soc.* **1997**, *119*, 6863–6872.

(76) Cortes, J.; Heitele, H.; Jortner, J. *J. Phys. Chem.* **1994**, *98*, 2527–2536.

(77) Kapturkiewicz, A.; Herbich, J.; Karpiuk, J. *J. Chem. Phys. A* **1997**, *101*, 2332–2344.

(78) Stahl, R.; Lambert, C.; Kaiser, C.; Wortmann, R.; Jakober, R. *Chem. Eur. J.* **2006**, *12*, 2358–2370.

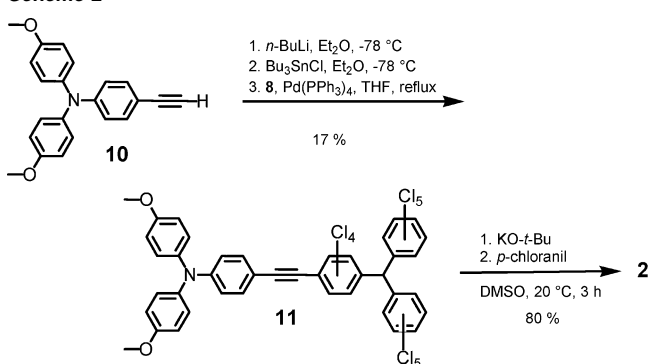
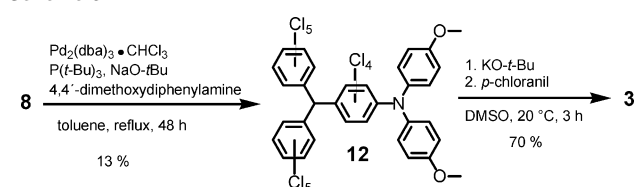
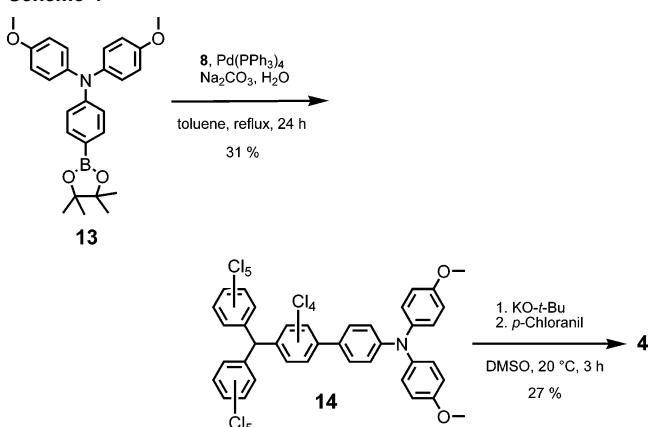
(79) Bässler, H.; Schweitzer, B. *Acc. Chem. Res.* **1999**, *32*, 173–182.

**Scheme 1**

amination. The synthesis of compound **8** was achieved by perchlorination reaction of **9**⁸⁰ with the so-called BMC method of Ballester et al.⁸¹ in good yield (Scheme 1).

The donor and acceptor units in **2** were linked by a Stille coupling⁸² of the terminal alkyne **10**⁸³ and the perchlorinated triarylmethane **8** (Scheme 2). The low yield may be due to the steric hindrance of **8**. Unfortunately, Hagihara–Sonogashira coupling reactions^{84,85} of **8** and **10** using different catalyst systems gave no better yields. Finally, the α -H compound **11** was transformed into the radical **2** as mentioned above (Scheme 2).

The synthesis of radical **3** is shown in Scheme 3. Starting from **8**, 4,4'-dimethoxydiphenylamine was directly connected to the perchlorinated ring system by a Pd-catalyzed Buchwald–Hartwig amination.^{86,87} Also in this case, the low yield could be traced back to the steric hindrance of **8**. After transformation into the radical, **3** can be isolated as an auburn solid (Scheme 3).

Scheme 2**Scheme 3****Scheme 4**

Radical **4**, in which the two redox centers are connected by a biphenyl spacer, was synthesized by a Suzuki coupling according to the literature.^{88,89} Starting from pinacole borane **13**,¹³ the radical precursor **14** was synthesized in 31% yield by a Pd-catalyzed Suzuki coupling with **8**. The somewhat better yield indicates that the Suzuki coupling is not as strongly affected by steric effects as the Stille, Hagihara–Sonogashira, or Buchwald–Hartwig coupling (Scheme 4).

Compounds **5** and **6** were both synthesized in a similar manner (Scheme 5). The terminal alkynes **15a**⁹⁰ and **15b**⁹⁰ were coupled to the perchlorinated triarylmethyl compound **8** by a Stille coupling reaction. The α -H compounds **16a** and **16b** were transformed to the corresponding radicals **5** and **6** as described above.

In Scheme 6, the synthesis of the dimethylamino-substituted perchlorinated radical **7** is sketched. The synthesis is straightforward and analogous to those of radicals **5** and **6**.

Electrochemistry. In order to investigate the redox properties of **1–7**, cyclic voltammograms (CVs) in dichloromethane/tetrabutylammonium hexafluorophosphate (TBAH) solution

(80) Brook, A. G.; Gilman, H.; Miller, L. S. *J. Am. Chem. Soc.* **1953**, *75*, 4759–4762.

(81) Ballester, M.; Castaner, J.; Riera, J.; Ibanez, A.; Pujadas, J. *J. Org. Chem.* **1982**, *47*, 259–264.

(82) Stille, J. K. *Angew. Chem.* **1986**, *98*, 504–519.

(83) Lin, J.-H.; Elangovan, A.; Ho, T.-I. *J. Org. Chem.* **2005**, *70*, 7397–7407.

(84) Thorand, S.; Krause, N. *J. Org. Chem.* **1998**, *63*, 8551–8553.

(85) Hundertmark, T.; Littke, A. F.; Buchwald, S. L.; Fu, G. C. *Org. Lett.* **2000**, *2*, 1729–1731.

(86) Harris, M. C.; Buchwald, S. L. *J. Org. Chem.* **2000**, *65*, 5327–5333.

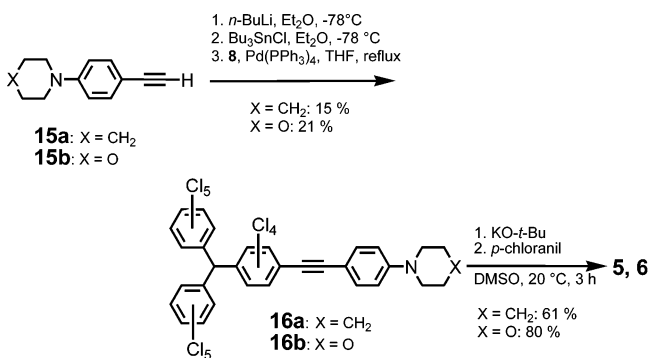
(87) Hartwig, J. F.; Kawatsura, M.; Hauck, S. I.; Shaughnessy, K. H.; Alcazar-Roman, L. M. *J. Org. Chem.* **1999**, *64*, 5575–5580.

(88) Miyaura, N.; Suzuki, A. *Chem. Rev.* **1995**, *95*, 2457–2483.

(89) Suzuki, A. *J. Organomet. Chem.* **1999**, *576*, 147–168.

(90) Elangovan, A.; Chen, T.-Y.; Chen, C.-Y.; Ho, T.-I. *Chem. Commun.* **2003**, 2146–2147.

Scheme 5



Scheme 6

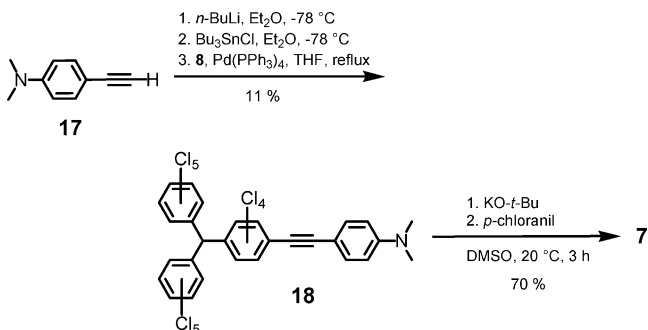


Table 1. Redox Potentials of Radicals **1–7** in Dichloromethane/0.1 M TBAH Solution with Fc/Fc⁺ as Reference

| | $E_{1/2}(\text{Red1})^a/\text{mV}$ | $E_{1/2}(\text{Ox1})^a/\text{mV}$ | $\Delta E/\text{mV}$ |
|----------|------------------------------------|-----------------------------------|----------------------|
| 1 | -670 | +240 | 910 |
| 2 | -590 | +315 | 905 |
| 3 | -650 | +445 | 1095 |
| 4 | -645 | +305 | 950 |
| 5 | -590 | +365 ^b | 955 |
| 6 | -580 | +455 ^b | 1035 |
| 7 | -570 | +385 ^{b,c} | 955 |

^a All values were determined with a maximum error of ± 5 mV. ^b Quasi-reversible under semi-infinite conditions but irreversible in thin-layer measurements. ^c Second oxidation at +540 mV.

were measured (Table 1). The chemical reversibility of all observed redox processes was also checked by thin-layer measurements. All donor-substituted compounds **1–7** show one reversible reduction process at about $E_{1/2} = -600$ mV vs ferrocene, which is assigned to the reduction of the triarylmethyl radical to the carbanion. Radicals **1–7** also show at least one oxidation signal, corresponding to the oxidation of the nitrogen center to the radical cation. This oxidation is reversible for all radicals **1–4** with dianisylamino moieties. A signal for the oxidation of the triarylmethyl radical center was not observed in any case up to +1000 mV potential. For the dialkyl-substituted radicals **5, 6**, and **7**, the amine-based oxidation is reversible under semi-infinite conditions only. We assume that α -H elimination processes are responsible for the instability of the generated radical cations. For radical **7** we observed a second oxidation signal that also is irreversible in thin-layer experiments.

The redox potentials of radicals **5–7** with constant spacer but varying donors show that the donor unit has no influence on the reduction of the radical center because of the large distance between the two redox centers. Owing to morpholine

being a weaker donor than piperidine or dimethylamine,^{90,91} the ΔE value of **6** is larger than that of **5** or **7**.

UV/Vis/NIR Spectroscopy. The UV/vis/NIR absorption spectra of **1–7** in dichloromethane are shown in Figure 2. In all spectra, an intense band A at ca. 25 500 cm⁻¹ can be observed which is assigned to a localized absorption of the perchlorinated ring system.^{81,92,93} Furthermore, all spectra show one or two weak absorption bands B and C at about 19 000 cm⁻¹, which are characteristic for PCTM radical systems.^{81,94} The absorption maxima $\tilde{\nu}_{\text{max}}$ and the corresponding extinction coefficients ϵ of these bands are summarized in Table 2. It is noteworthy that, for **3** and **4**, the radical bands B and C are very weak, which is obviously due to the lack of either alkenyl or alkynyl spacer units.

The absorption bands in the NIR region at ca. 12 000 cm⁻¹ are the focus of our interest. These bands can be assigned to an optically induced ET from the donor center to the triarylmethyl radical unit. As can be seen from Figure 2 and Table 3, the extinction coefficients of all these IV-CT bands are similar, except for radical **4**, which shows a much weaker IV-CT band intensity. This indicates a much lower electronic communication between the two redox centers as a result of a twist of the aromatic biphenyl spacer unit caused by the di-*ortho*-substitution of one benzene subunit.⁹⁵ In radical **3**, a related effect might be compensated by the shorter distance between the two redox centers.

The neutral character of compounds **1–7** and their excellent solubility gave us the chance to investigate the IV-CT bands in 13 solvents of different polarity, ranging from totally nonpolar (*n*-hexane) to strongly polar (acetonitrile). All compounds show a weak but superficially nonsystematic dependence of $\tilde{\nu}_{\text{max}}$ on the solvent polarity. On the other hand, we observed a systematic dependence of the band shape on the polarity of the solvent, i.e., higher extinction coefficients and smaller bandwidths at half-height $\tilde{\nu}_{1/2}$ in nonpolar solvents such as cyclohexane than in polar solvents like acetonitrile (Figure 3). Furthermore, the IV-CT bands show a more or less intense vibronic fine structure in nonpolar solvents like the hexanes.

In order to understand this behavior, we applied Jortner's model (eq 6) to fit the IV-CT bands in each solvent by varying the parameters for the inner reorganization energy λ_{v} and the solvent reorganization energy λ_{o} , as well as the parameters of the difference in the free energy between the diabatic ground and excited states ΔG^{oo} and the average molecular vibrational mode $\tilde{\nu}_{\text{v}}$. In this way, we achieved an excellent least-squares fit of the IV-CT bands of compounds **1, 2**, and **5–7** (see Figure 4 for a typical example).

However, we were unable to fit the IV-CT band of radical **4** in polar solvents because the bands are too symmetrical to obtain a fit with acceptable maximum errors. For the fit of radical **3**,

- (91) Effenberger, F.; Fischer, P.; Schoeller, W. W.; Stohrer, W.-D. *Tetrahedron* **1978**, *34*, 2409–2417.
- (92) Veciana, J.; Armet, O.; Rovira, C.; Riera, J.; Castaner, J.; Molins, E.; Rius, J.; Miravittles, C.; Olivella, S.; Brichfeus, J. *J. Phys. Chem.* **1987**, *91*, 5608–5616.
- (93) Ballester, M.; Riera, J.; Castaner, J.; Badia, C.; Monso, J. M. *J. Am. Chem. Soc.* **1971**, *93*, 2215–2225.
- (94) The UV/vis/NIR spectra of **16a**, **16b**, and **18** show no absorption in this region, so we can exclude that the bands at ca. 21 500 cm⁻¹ are due to an absorption associated with the morpholine, piperidine, or dimethylamino moieties.
- (95) Low, P. J.; Paterson, M. A. J.; Goeta, A. E.; Yufit, D. S.; Howard, J. A. K.; Cheryman, J. C.; Tackley, D. R.; Brown, B. *J. Mater. Chem.* **2004**, *14*, 2516–2523.

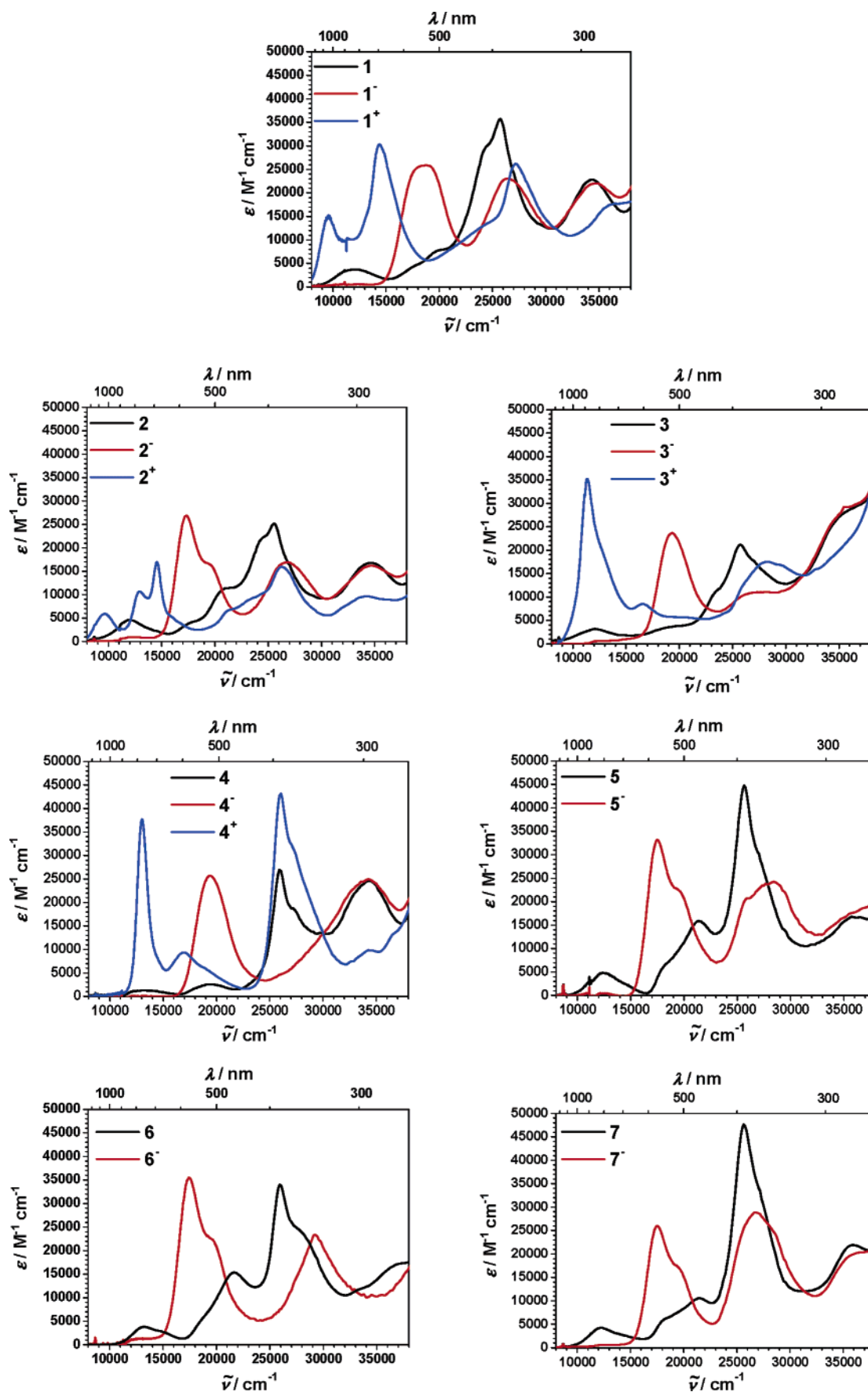


Figure 2. UV/vis/NIR absorption spectra of radicals 1–7 (black) and of the corresponding anions (red) and cations (blue) in dichloromethane generated by spectroelectrochemistry.

Table 2. Absorption Maxima and Extinction Coefficients of Bands A, B, and C of **1–7** in Dichloromethane

| | $\bar{\nu}/\text{cm}^{-1}$ ($\epsilon/M^{-1}\text{cm}^{-1}$) | | |
|----------|--|----------------------------|---------------------------|
| | band A | band B | band C |
| 1 | 25700 (35800) | 20000 (7700) | 17800 (4600) |
| 2 | 25600 (25300) | 21200 (11500) ^a | 17800 (4200) ^a |
| 3 | 25800 (21300) | 19800 (3800) ^a | |
| 4 | 25600 (27000) | 19400 (2700) | |
| 5 | 25600 (44700) | 21400 (16000) | 18200 (6700) ^a |
| 6 | 25900 (33900) | 21700 (15400) | |
| 7 | 25600 (47600) | 21500 (10500) | 18200 (6100) ^a |

^a Shoulder.

the same problems appeared but in an alleviated form. The symmetry and, as a consequence thereof, the problems in fitting the IV-CT bands of **3** and **4** can be traced back to a high Huang–Rhys factor S . We assume that the lack of an unsaturated C–C bridge unit in **3** and **4** causes a lower average vibrational mode $\bar{\nu}_v$, which makes S high and the IV-CT bands symmetrical. The vibronic fine structure of the IV-CT bands in nonpolar solvents mentioned above is a consequence of the low solvent reorganization energy λ_o compared to the average molecular vibrational mode $\bar{\nu}_v$. The data of all fits are summarized in Table 3.

It is apparent from the data in Table 3 that the Marcus reorganization energy is dominated by the solvent part, except for the very nonpolar solvents *n*-hexane and cyclohexane. A plot of each parameter vs the Onsager solvent polarity function $(D - 1)/(2D + 1) - (n^2 - 1)/(2n^2 + 1)$, where D is the permittivity and n the refractive index, reveals linear correlations for both ΔG° and λ_o with solvent polarity (for comments about the use of the polarity function, see the Appendix in the Supporting Information). In Figure 5 the correlations are plotted and the data points for compound **2** only are shown for clarity. The scatter of data for the other compounds is similar.

As expected from Marcus theory,⁹⁶ the solvent reorganization energies λ_o increase with solvent polarity and approach zero for totally apolar environments (Figure 5b). Concomitantly, the values for ΔG° decrease due to the fact that the excited states of **1–7** have zwitterionic character while the ground states possess a small dipole moment⁷¹ (Figure 5a). Thus, the weak and unsystematic solvent dependence of the IV-CT bands is a result of these two compensating trends. Consequently, the positive solvatochromism which is expected for chromophores with small ground-state dipole moment and large excited-state dipole moment is not observed. The plots also prove the independence of the vibrational reorganization energy λ_v on the solvent polarity (Figure 5c). However, we also recorded a weak but systematic dependence of the average molecular vibrational mode $\bar{\nu}_v$ on solvent polarity (Figure 5d), which could be a result of the varying importance of different molecular modes contributing to the averaged mode $\bar{\nu}_v$. However, it might also be that this shift compensates inaccuracies of the theory in general. It is noteworthy that for all compounds with an alkynyl spacer unit, $\bar{\nu}_v$ is noticeably higher (average 700 cm^{-1}) than for compound **1**, with an alkenyl spacer, and radical **3**, with no unsaturated spacer unit. This energy difference is due to an alkynyl vibrational mode having typically more energy than an alkenyl or a C–C single bond vibrational mode. This is, to our

knowledge, the first time that a difference in averaged molecular mode $\bar{\nu}_v$ can directly be assigned to a molecular parameter, i.e., C=C double bond vs C≡C triple bond.⁹⁷

Estimation of Electronic Coupling V_{12} . As we outlined in the Introduction, estimation of the electronic coupling V_{12} via eqs 2 and 4 requires knowledge of the diabatic dipole moment difference $\Delta\mu_{ab}$. Quite recently, we evaluated this dipole moment difference for **1** by EOAM, which yielded 19 ± 1 D.⁷¹ Here we apply a quite different and much less laborious methodology which is based on the evaluation of band shape parameters only: according to Lippert and Mataga,^{98,99} the difference in absorption and fluorescence energy can be correlated with the Onsager solvent parameter as given in eq 7, with the assumption of a spherical chromophore geometry with radius a_0 (for a derivation of eq 7, see the Appendix in the Supporting Information). Based on a purely classical model (with parabolic potentials for the ground and the excited states), the total reorganization energy λ is given by eq 8.¹⁰⁰

$$2(\lambda_v + \lambda_o) = \bar{\nu}_{\text{abs}} - \bar{\nu}_{\text{fl}} = \frac{(\Delta\mu_{ab})^2}{2\pi\epsilon_0\hbar c a_0^3} (f(D) - f(n^2)) + (\bar{\nu}_{\text{abs}}^{\text{gas}} - \bar{\nu}_{\text{fl}}^{\text{gas}}) \quad (7)$$

$$\text{with} \quad f(D) = \frac{D-1}{2D+1} \quad \text{and} \quad f(n^2) = \frac{n^2-1}{2n^2+1}$$

$$\lambda_v + \lambda_o = \frac{\bar{\nu}_{\text{abs}} - \bar{\nu}_{\text{fl}}}{2} \quad (8)$$

Consequently, plots of $2(\lambda_v + \lambda_o)$ (values taken from the Jortner fits above) vs the Onsager solvent parameter $f(D) - f(n^2)$ for MV compounds **1–3** and **5–7** in a broad variety of solvents (Figure 6) and linear fits (Figure 6) of these plots yield the adiabatic dipole moment differences $\Delta\mu_{ab}$ from the slope. The radii a_0 of all compounds, which are necessary input into eq 7, were determined by calculating the Connolly solvent-excluded volume of the molecules¹⁰¹ and then assuming that the compounds have spherical geometry.

With the data for the adiabatic dipole moment differences obtained in the above-mentioned way, we were able to calculate the diabatic dipole moment differences $\Delta\mu_{12}$ between the ground and the excited states by eq 4. The corresponding values for the electronic coupling V_{12} were determined by using eq 2. The data for all compounds **1–3** and **5–7** are summarized in Table 4. The good agreement of the dipole moment difference $\Delta\mu_{ab}$ of **1** (17.6 D) derived by the solvatochromic method above with the value obtained recently by EAOM (19 ± 1 D)⁷¹ shows that our new solvatochromic method described here is well suitable to yield reliable dipole moment differences, comparable to those obtained by the much more complicated EAOM method.

It is apparent from the data in Table 4 that the electronic coupling values V_{12} of all compounds **1–3** and **5–7** are within a narrow range of about 2300–3000 cm^{-1} and the solvent dependence of V_{12} is also quite small. The electronic coupling

(96) Brunshwig, B. S.; Ehrenson, S.; Sutin, N. *J. Phys. Chem.* **1986**, *90*, 3657–3668.

(97) Kjaer, A. M.; Ulstrup, J. *J. Am. Chem. Soc.* **1987**, *109*, 1934–1942.

(98) Mataga, N.; Kaifu, Y.; Koizumi, M. *Bull. Chem. Soc. Jpn.* **1956**, *29*, 465–470.

(99) Lippert, E. Z. *Elektrochem.* **1957**, *61*, 962–975.

(100) Brunshwig, B. S.; Ehrenson, S.; Sutin, N. *J. Phys. Chem.* **1987**, *91*, 4714–4723.

(101) *CS Chem3D Pro*; CambridgeSoft Corp.: Cambridge, MA, 1999.

Table 3. Absorption Maxima, Extinction Coefficients, and Resulting ET Parameters of the Least-Squares Fits of the IV-CT Bands of **1–7** in Solvents of Different Polarity

| | $\tilde{\nu}_{\max}$ cm ⁻¹ | ϵ / M ⁻¹ cm ⁻¹ | $\Delta G^{\circ 0}$ / cm ^{-1 a} | λ_{off} / cm ^{-1 a} | λ_{off} / cm ^{-1 a} | $\tilde{\nu}_{\text{off}}$ / cm ^{-1 a} | | $\tilde{\nu}_{\max}$ cm ⁻¹ | ϵ / M ⁻¹ cm ⁻¹ | $\Delta G^{\circ 0}$ / cm ^{-1 a} | λ_{off} / cm ^{-1 a} | λ_{off} / cm ^{-1 a} | $\tilde{\nu}_{\text{off}}$ / cm ^{-1 a} |
|------------------------------|--|--|--|--|--|--|------------------|--|--|--|--|--|--|
| Radical 1 | | | | | | | Radical 5 | | | | | | |
| <i>n</i> -hexane | 12400 | 4750 | 10250 | 1000 | 1250 | 1150 | <i>n</i> -hexane | 13550 | 5300 | 11550 | 1250 | 1050 | 1700 |
| cyclohexane | 12250 | 4600 | 10200 | 1050 | 1100 | 1200 | cyclohexane | 13450 | 5100 | 11350 | 1300 | 1050 | 1700 |
| 1,4-dioxane | 12200 | 3900 | 9450 | 1850 | 1650 | 1400 | 1,4-dioxane | 13100 | 5000 | 10050 | 2400 | 950 | 2000 |
| dibutyl ether | 11950 | 4150 | 9250 | 1700 | 1200 | 1400 | dibutyl ether | 13050 | 4850 | 10050 | 2350 | 950 | 2050 |
| diethyl ether | 12000 | 4050 | 8850 | 2050 | 1350 | 1450 | diethyl ether | 13000 | 5250 | 9600 | 2700 | 900 | 2100 |
| MTBE | 12000 | 3650 | 8750 | 2200 | 1300 | 1450 | MTBE | 12950 | 5150 | 9450 | 2900 | 900 | 2150 |
| ethyl acetate | 11900 | 3850 | 8050 | 2900 | 1250 | 1650 | ethyl acetate | 12650 | 5250 | 8100 | 4150 | 850 | 2550 |
| THF | 11750 | 3550 | 7500 | 3350 | 1100 | 1750 | THF | 12650 | 5300 | 8250 | 3750 | 800 | 2350 |
| dichloromethane | 12150 | 3600 | 8100 | 3000 | 1400 | 1550 | dichloromethane | 12800 | 4900 | 8900 | 3300 | 900 | 2200 |
| benzonitrile | 11650 | 3600 | 7300 | 3400 | 1150 | 1700 | benzonitrile | 12650 | 5700 | 8550 | 3500 | 850 | 2300 |
| 2-propanol | 11800 | 3900 | 8100 | 2750 | 1200 | 1650 | 2-propanol | 12750 | 5100 | 8550 | 3500 | 850 | 2250 |
| acetone | 11950 | 3550 | 6550 ^b | 4750 ^b | 1050 | 2000 ^b | acetone | 12600 | 5050 | 7750 | 4350 | 800 | 2500 |
| acetonitrile | 12200 | 3400 | 7250 ^b | 4150 ^b | 1350 | 1750 | acetonitrile | 12750 | 4550 | 7900 | 4400 | 800 | 2500 |
| Radical 2 | | | | | | | Radical 6 | | | | | | |
| <i>n</i> -hexane | 12650 | 8150 | 10900 | 1050 | 650 | 1650 | <i>n</i> -hexane | 14200 | 3800 | 12350 | 1050 | 1200 | 1650 |
| cyclohexane | 12400 | 7250 | 10600 | 1150 | 650 | 1650 | cyclohexane | 13950 | 3800 | 12150 | 1150 | 1200 | 1700 |
| 1,4-dioxane | 12400 | 5800 | 9400 | 2550 | 650 | 2250 | 1,4-dioxane | 13600 | 3500 | 11000 | 2000 | 1100 | 1950 |
| dibutyl ether | 12200 | 7050 | 9500 | 2200 | 600 | 2100 | dibutyl ether | 13600 | 4300 | 11100 | 1900 | 1100 | 1950 |
| diethyl ether | 12200 | 6400 | 8800 | 2900 | 600 | 2400 | diethyl ether | 13550 | 4100 | 10700 | 2250 | 1050 | 2000 |
| MTBE | 12200 | 6400 | 8850 | 2900 | 600 | 2350 | MTBE | 13500 | 3950 | 10650 | 2300 | 1100 | 2000 |
| ethyl acetate | 12200 | 6000 | 8150 | 3650 | 600 | 2650 | ethyl acetate | 13300 | 4250 | 9600 | 3250 | 1050 | 2300 |
| THF | 12000 | 5550 | 7650 | 3950 | 650 | 3050 | THF | 13200 | 3650 | 9250 | 3450 | 1200 | 2550 |
| dichloromethane | 12300 | 5000 | 8300 | 3600 | 650 | 2600 | dichloromethane | 13550 | 3509 | 10500 | 2450 | 1100 | 2050 |
| benzonitrile | 11850 | 5250 | 6800 | 4750 | 650 | 3950 ^b | benzonitrile | 13100 | 3650 | 8800 | 3850 | 1050 | 2800 |
| 2-propanol | 12000 | 5800 | 8250 | 3350 | 550 | 2550 | 2-propanol | 13300 | 3900 | 9750 | 3050 | 1000 | 2200 |
| acetone | 12200 | 5400 | 7550 | 4300 | 600 | 2950 | acetone | 13250 | 3900 | 9100 | 3700 | 950 | 2400 |
| acetonitrile | 12450 | 5400 | 7900 | 4200 | 650 | 2800 | acetonitrile | 13400 | 4050 | 9500 ^b | 3450 ^b | 1050 | 2300 |
| Radical 3 | | | | | | | Radical 7 | | | | | | |
| <i>n</i> -hexane | 12050 | 5050 | 9650 | 1650 | 800 | 1300 | <i>n</i> -hexane | 13400 | 4600 | 11900 | 800 | 950 | 1600 |
| cyclohexane | 11950 | 4600 | 9600 | 1450 | 850 | 1200 | cyclohexane | 13300 | 4700 | 11750 | 750 | 900 | 1550 |
| 1,4-dioxane | 11900 | 4150 | 8350 | 2950 | 650 | 1500 | 1,4-dioxane | 12950 | 3650 | 10400 | 1900 | 900 | 2050 |
| dibutyl ether | 11750 | 4350 | 8500 | 2650 | 650 | 1500 | dibutyl ether | 12900 | 4300 | 10550 | 1700 | 900 | 2000 |
| diethyl ether | 11750 | 4750 | 7900 | 3350 | 550 | 1650 | diethyl ether | 12800 | 4250 | 9950 | 2250 | 900 | 2150 |
| MTBE | 11750 | 4300 | 8100 | 3050 | 650 | 1450 | MTBE | 12800 | 3950 | 9950 | 2250 | 900 | 2150 |
| ethyl acetate | 11750 | 4050 | 7750 | 3300 | 700 | 1400 | ethyl acetate | 12650 | 3950 | 9000 | 3050 | 950 | 2500 |
| THF | 11650 | 3850 | 7250 | 3850 | 500 | 1950 | THF | 12450 | 3950 | 8850 | 3000 | 800 | 2450 |
| dichloromethane | 12050 | 3700 | 7350 | 4450 | 450 | 2000 | dichloromethane | 12150 | 3850 | 9450 | 2650 | 850 | 2250 |
| benzonitrile | 11600 | 3450 | 7200 | 3800 ^b | 650 | 1400 | benzonitrile | 12250 | 3550 | 8550 | 3050 | 750 | 2450 |
| 2-propanol ^c | 11600 | 3950 | | | | | 2-propanol | 12550 | 3450 | 9050 | 2900 | 850 | 2450 |
| acetone | 11800 | 3400 | 7450 | 3450 ^b | 900 | 1200 | acetone | 12500 | 3400 | 8450 | 3500 | 850 | 2500 |
| acetonitrile ^c | 11900 | 3550 | | | | | acetonitrile | 12650 | 3700 | 8400 | 3700 | 900 | 2600 |
| Radical 4 | | | | | | | | | | | | | |
| <i>n</i> -hexane | 13200 | 1400 | 10350 ^b | 2350 ^b | 700 | 1600 ^b | | | | | | | |
| cyclohexane | 13050 | 1300 | 10600 | 1600 | 900 | 1250 | | | | | | | |
| 1,4-dioxane ^c | 13250 | 1050 | | | | | | | | | | | |
| dibutyl ether | 12900 | 1200 | 7900 | 4700 ^b | 500 | 2450 ^b | | | | | | | |
| diethyl ether | 13000 | 1100 | 7600 | 5000 ^b | 550 | 1950 ^b | | | | | | | |
| MTBE ^c | 12950 | 1050 | | | | | | | | | | | |
| ethyl acetate ^c | 13250 | 1100 | | | | | | | | | | | |
| THF ^c | 12850 | 1000 | | | | | | | | | | | |
| dichloromethane ^c | 13150 | 1050 | | | | | | | | | | | |
| benzonitrile ^c | 13000 | 950 | | | | | | | | | | | |
| 2-propanol ^c | 13050 | 1000 | | | | | | | | | | | |
| acetone ^c | 13200 | 950 | | | | | | | | | | | |
| acetonitrile ^c | 13450 | 1000 | | | | | | | | | | | |

^a All values were determined with a maximum error of ± 50 cm⁻¹. ^b All values were determined with a maximum error of ± 150 cm⁻¹. ^c No fit was possible because of a too large maximum error of > 150 cm⁻¹.

of **3** is about the same as that of **2**, which supports our assumption made above, that the smaller ET distance (demonstrated by the smaller $\Delta\mu_{\text{ab}}$ value) is compensated by a smaller transition moment which is due to the weakening of electronic coupling, presumably by torsional effects. Comparison of V_{12} of **1** and of **2** shows that of the latter to be significantly higher by ca. 280 cm⁻¹. This is in contrast to the behavior observed in analogous bis(triarylamine) radical cations with alkynyl and alkenyl bridges, where the electronic coupling is somewhat

larger in the alkenyl system.^{22,71,102} This effect might also be explained by twisting of the alkenyl group due to steric interactions with *ortho*-chloro atoms.

UV/Vis/NIR Spectroelectrochemistry. In order to probe the spectral changes that result upon charging the compounds, the UV/vis/NIR absorption spectra of **1–7** upon oxidation to the monocations, as well as upon reduction to the monoanions, were

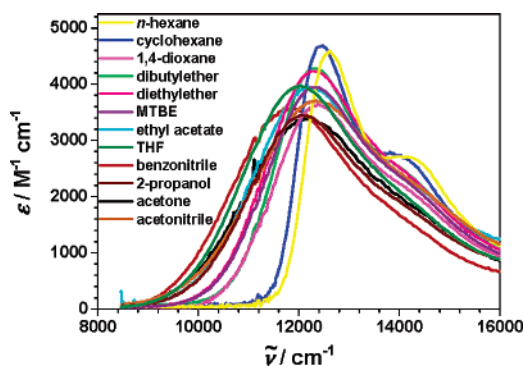


Figure 3. IV-CT bands of **7** in solvents of different polarity. MTBE = methyl *tert*-butyl ether.

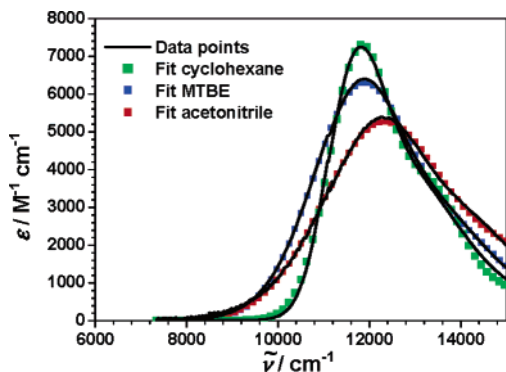


Figure 4. Least-squares fits of the IV-CT bands of **2** in solvents of different polarity.

investigated by spectroelectrochemistry in dichloromethane solutions. While for all radicals **1–7** the spectra of the corresponding monoanions **1[–]–7[–]** could be generated, only the monocations **1⁺–4⁺** with dianisyl moieties could be investigated, because **5–7** undergo irreversible oxidation to their monocations. As can be seen from Figure 2, the IV-CT band of all radicals disappears upon reduction, and no absorptions in the NIR region are observed due to the fact that the monoanions are not mixed valent. This behavior also proves the NIR bands of the neutral compounds **1–7** to be IV-CT bands. At the same time, a new intense band D at around 19 500 cm^{-1} is visible, which we assign to an absorption of the PCTM carbanion moiety in **1[–]–7[–]**.^{25,49} For all systems with alkynyl or alkenyl spacers, this band partially overlaps with a second, even more intense band E at around 17 500 cm^{-1} . Furthermore, a decrease in band A can be observed, associated with reduction of the carbon radical center; additionally, the typical radical bands B and C decrease, which can be seen in the spectra of carbanions **5[–]–7[–]** (Figure 2). The data of all the bands discussed for the monoanions are summarized in Table 5.

The spectra of radical cations **1⁺–4⁺** in dichloromethane generated by spectroelectrochemistry are also displayed in Figure 2 (blue solid lines). All cations show intense absorption signals (F and G) in the region at ca. 13 000–14 500 cm^{-1} which can be assigned to the oxidation of the triarylamine moiety to the corresponding radical cations (Table 6).¹⁰³ Furthermore, a relatively intense band (H) at ca. 9600 cm^{-1} increases upon oxidation of radicals **1** and **2**. This band can be traced back to an optically induced IV-CT process in the cations

1⁺ and **2⁺**, which can also be conceived as donor–acceptor compounds (Figure 7) in which the triarylmethyl and triarylamine moieties of **1** and **2** exchanged their donor and acceptor properties.

It is noteworthy that only in the absorption spectra of cations **1⁺** and **2⁺**, with an unsaturated bridge unit, band H can be observed, while compounds **3⁺** and **4⁺** do not show any comparable absorption band. Instead, a very intense band G is visible which might hide a potentially blue-shifted IV-CT band at the red edge. Furthermore, band F is less intense and blue-shifted in **3⁺** and **4⁺** compared to **1⁺** and **2⁺**.

Conclusions

Our concept to combine perchlorinated triarylmethyl radical acceptors with nitrogen donor centers yields the neutral, purely organic MV compounds **1–7**. This new class of organic molecules, which are isoelectronic to the well-established bis-(triarylamine) radical cations, show several unique properties which allow a straightforward and detailed study of the charge-transfer behavior of these compounds by all-optical measurements. The neutral character and, consequently, the excellent solubility of the MV compounds **1–7** allowed the investigation of the ET behavior in both polar and nonpolar solvents and offered the unique chance to study the solvatochromic behavior of these compounds by UV/vis/NIR spectroscopy. All radicals **1–7** show a characteristic IV-CT band at 11 000–13 000 cm^{-1} with a weak but nonsystematic solvatochromic behavior. However, by applying Jortner's model, we achieved excellent least-squares fits of the IV-CT bands of all MV compounds in each solvent except for compound **4** and, in an alleviated form, for radical **3**. In these compounds, the lack of an unsaturated bridge unit finally causes the Huang–Rhys factor *S* to be too high, which in turn is the reason for symmetrical IV-CT bands. With the aid of the Jortner fits, we were able to evaluate reliable values for the inner reorganization energy λ_v and the solvent reorganization energy λ_o , as well as values for the free energy ΔG° and the averaged molecular vibrational modes $\bar{\nu}_v$ in each solvent separately. Plots of each parameter vs the Onsager solvent parameter revealed that the missing visible solvatochromic behavior is the result of two opposing effects, a positive solvatochromism of ΔG° and a negative solvatochromism of λ_o . The plots also proved the independence of the inner reorganization energy λ_v on the solvent polarity. Furthermore, the plots show that the values of the averaged vibrational modes of radicals **1** and **5–7** with a spacer containing a C≡C triple bond are distinctly higher than the values determined for radicals **2** and **3**, where the triple bond is absent. This is the first time that molecular parameters can be directly associated with differences in averaged molecular modes, and this work demonstrates the usefulness of the band shape analysis in the context of Jortner's model.

The separately determined values for λ_o and λ_v allowed a plot of $2(\lambda_o + \lambda_v)$ vs the Onsager solvent parameter according to Lippert and Mataga. By a linear fit of this plot, we were able to determine the adiabatic dipole moment difference $\Delta\mu_{12}$. This dipole moment difference is in excellent agreement with that obtained by an EAOM measurement. This new variant of dipole moment determination made an all-optical evaluation of the electronic coupling V_{12} possible. Moreover, the solvatochromic method outlined here is much simpler than the more

(103) Amthor, S.; Noller, B.; Lambert, C. *Chem. Phys.* **2005**, *316*, 141–152.

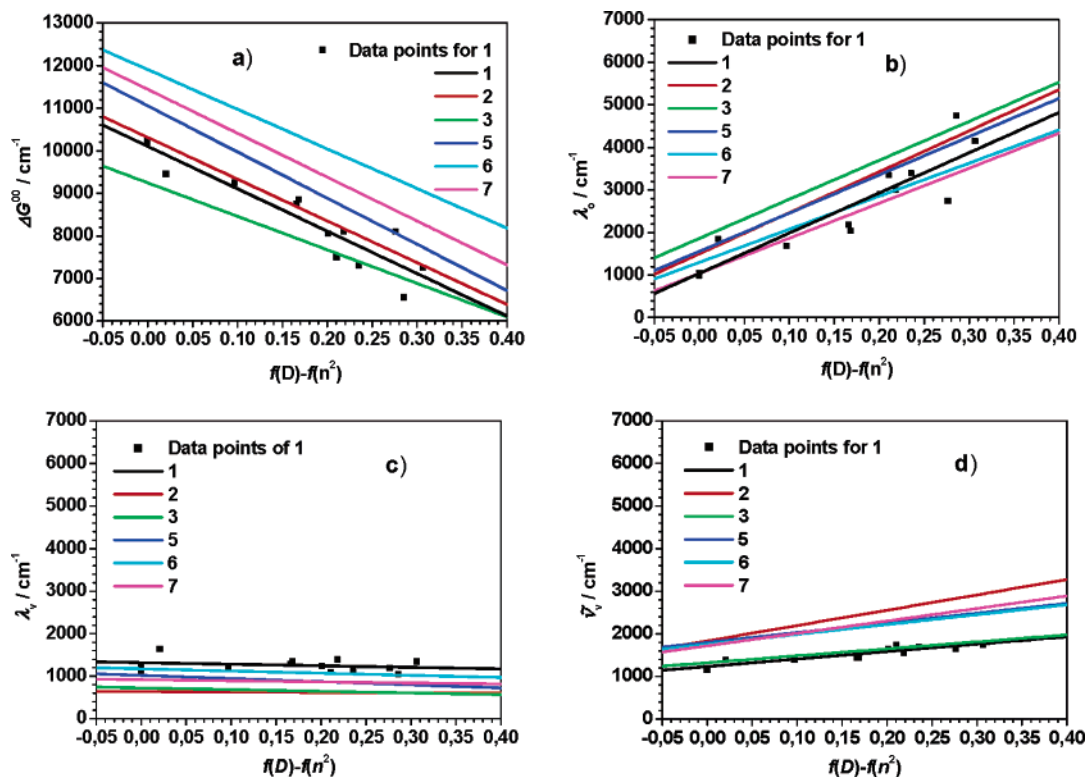


Figure 5. Linear correlations of (a) ΔG° , (b) λ_o , (c) λ_v , and (d) $\bar{\nu}_v$ versus the solvent polarity function $f(D) - f(n^2)$, with $f(D) = (D - 1)/(2D + 1)$ and $f(n^2) = (n^2 - 1)/(2n^2 + 1)$ for compounds 1–3 and 5–7. For simplicity, only the data points for 1 are shown.

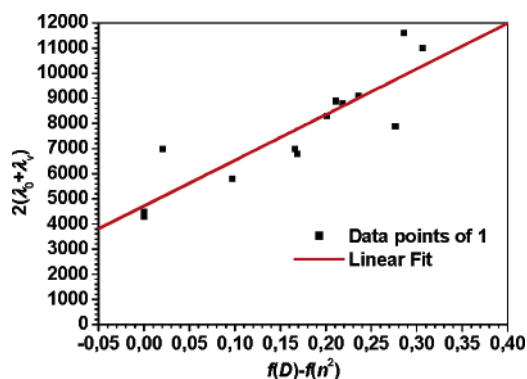


Figure 6. Plot of $2(\lambda_v + \lambda_o)$ vs the Onsager solvent parameter $f(D) - f(n^2)$ for radical 1 and linear fit. The values for the reorganization energies were taken from Table 3.

complex and time-consuming EOAM method or the methods based on quantum chemical calculations of the effective charge-transfer distance, which is often afflicted by major inaccuracies inherent in the theoretical approaches. While the straightforward application of Jortner's theory in combination with the Lippert–Mataga method to investigate the ET transfer behavior is, in principle, not restricted to neutral compounds, it is the uncharged character of neutral MV compounds which makes the analysis in a broad variety of solvents so simple. Thus, the new class of organic PCTM-donor molecules presents an almost perfect model system for the investigation of electron-transfer processes.

We also performed a detailed study of both the UV/vis/NIR absorption spectra of the carbanions 1^- – 7^- and the spectra of the diradical cations 1^+ – 4^+ obtained by spectroelectrochemical measurements. Thereby, the optically induced charge transfer of compounds 1–7 was proved by the absence of the IV-CT band upon reduction to the corresponding carbanions. The

absorption spectra of compounds 1^+ and 2^+ , with an unsaturated bridge unit, show the rise of a new intense band in the NIR region which can be assigned to intramolecular charge-transfer processes from the carbon radical centers to the nitrogen radical cation centers. Thus, compounds 1 and 2 show, both in the neutral state and in the oxidized state, a charge-transfer behavior but with exchanged donor and acceptor functionalities. A detailed study of this remarkable behavior, which until now was observed only in neutral MV compounds, is the focus of further investigations in our laboratories.

Experimental Section

Cyclic Voltammetry and Spectroelectrochemistry. The electrochemical measurements were performed in a 0.1 M solution of TBAH as supporting electrolyte in dry, argon-saturated CH_2Cl_2 under an argon atmosphere. The concentration of the substrates was 0.1 mM. All potentials were referenced vs ferrocene (Fc/Fc^+). The spectroelectrochemical measurements were carried out with the solutions of the CV experiments that were transferred into a thin-layer cell with a gold minigrid working electrode. The design of the cell was described elsewhere;¹⁰⁴ the optical path length was 100 μm . All UV/vis/NIR spectra were recorded with a Jasco V-570 UV/vis/NIR spectrophotometer in transmission mode.

Mass Spectroscopy. The ESI-TOF mass spectra were obtained with a Bruker Daltonics micrOTOF focus mass spectrometer equipped with an APCI ion source (Agilent G1947-60101). A stainless steel spraying capillary and, as transfer capillary, a nickel-coated glass capillary with an inner diameter of 500 μm were used. Due to the isotopic distribution over a broad m/z region caused by chlorine and/or bromine, the monoisotopic signals were too small in intensity for some compounds for an accurate mass measurement. In those cases, typically the most intense signal ($X + n$) of this isotopic distribution was taken and compared with the calculated value. For calculation of the mass values

Table 4. Connolly Solvent-Excluded Volume V_{Con} , Radii of the Molecules a_0 , Diabatic Dipole Moment Difference $\Delta\mu_{\text{ab}}$, Transition Moment μ_{ab} , Adiabatic Dipole Moment Difference $\Delta\mu_{12}$, and Electron Coupling V_{12} of Radicals 1–7 in *n*-Hexane and Acetonitrile

| | | $V_{\text{Con}}/\text{\AA}^3$ | $a_0/\text{\AA}$ | $\Delta\mu_{\text{ab}}/\text{D}$ | $\mu_{\text{ab}}/\text{D}^a$ | $\Delta\mu_{12}/\text{D}$ | V_{12}/cm^{-1} |
|---|------------------|-------------------------------|------------------|----------------------------------|------------------------------|---------------------------|-------------------------|
| 1 | <i>n</i> -hexane | 718.4 | 5.56 | 17.6 ± 1.3 | 3.6 | 19.0 ± 1.7 | 2350 ± 230 |
| | MeCN | | | | 3.6 | 19.0 ± 1.7 | 2310 ± 230 |
| 2 | <i>n</i> -hexane | 710.4 | 5.54 | 17.9 ± 1.4 | 4.1 | 19.7 ± 1.6 | 2630 ± 240 |
| | MeCN | | | | 4.1 | 19.7 ± 1.6 | 2590 ± 230 |
| 3 | <i>n</i> -hexane | 698.2 | 5.50 | 15.4 ± 1.3 | 3.7 | 17.1 ± 1.6 | 2610 ± 270 |
| | MeCN | | | | 3.3 | 16.8 ± 1.5 | 2340 ± 230 |
| 5 | <i>n</i> -hexane | 605.6 | 5.25 | 15.4 ± 1.1 | 3.7 | 17.1 ± 1.3 | 2930 ± 240 |
| | MeCN | | | | 3.9 | 17.3 ± 1.3 | 2870 ± 240 |
| 6 | <i>n</i> -hexane | 592.8 | 5.21 | 14.3 ± 1.0 | 2.9 | 15.4 ± 1.3 | 2670 ± 250 |
| | MeCN | | | | 3.4 | 15.8 ± 1.3 | 2880 ± 260 |
| 7 | <i>n</i> -hexane | 564.0 | 5.13 | 14.6 ± 0.9 | 3.1 | 15.9 ± 1.1 | 2610 ± 200 |
| | MeCN | | | | 3.5 | 16.2 ± 1.1 | 2730 ± 200 |

^a All values were determined with a maximum error of ± 0.15 D.

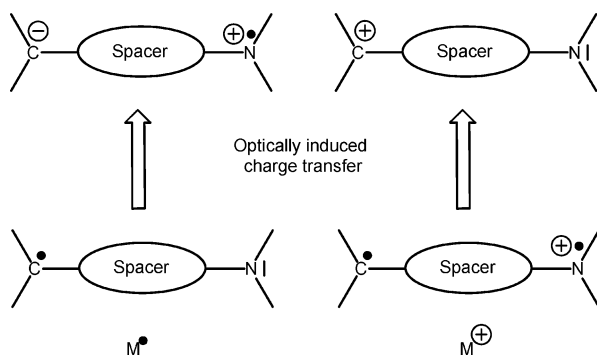
Table 5. Absorption Maxima and Extinction Coefficients of Bands D and E in the Absorption Spectra of Carbanions 1⁻–7⁻ in Dichloromethane

| | $\tilde{\nu}/\text{cm}^{-1}$ ($\epsilon/M^{-1}\text{cm}^{-1}$) | |
|----------------|--|---------------|
| | band D | band E |
| 1 ⁻ | 18900 (25800) ^a | 18200 (25700) |
| 2 ⁻ | 19500 (16600) ^a | 17300 (26900) |
| 3 ⁻ | 19300 (23600) | |
| 4 ⁻ | 19100 (25700) | |
| 5 ⁻ | 19600 (22400) ^a | 17500 (33200) |
| 6 ⁻ | 19700 (22300) ^a | 17400 (35500) |
| 7 ⁻ | 19500 (17100) ^a | 17500 (26000) |

^a Shoulder.

Table 6. Absorption Maxima and Extinction Coefficients of Bands F, G, and H in the Absorption Spectra of Cations 1⁺–4⁺ in Dichloromethane

| | $\tilde{\nu}/\text{cm}^{-1}$ ($\epsilon/M^{-1}\text{cm}^{-1}$) | | |
|----------------|--|---------------|--------------|
| | band F | band G | band H |
| 1 ⁺ | 14400 (30300) | | 9600 (15100) |
| 2 ⁺ | 14500 (16700) | 12900 (10700) | 9700 (5900) |
| 3 ⁺ | 16500 (8500) | 11400 (35200) | |
| 4 ⁺ | 16900 (9300) | 13000 (37700) | |

**Figure 7.** Optically induced ET of neutral MV compounds to a zwitterionic excited state (left-hand side) and optically induced hole transfer of the oxidized MV compounds (right-hand side).

of the isotopic distribution, the software module “Bruker Daltonics IsotopePattern” of the software Compass 1.1 (Bruker Daltonik GmbH, Bremen, Germany) was used.

GP1: General Procedure for the Radical Formation of α -H Compounds. The α -H compound (1.00 equiv) was dissolved in dry DMSO (1 mL per 100 μmol of α -H compound) under an inert gas atmosphere. KO-*t*Bu (2.00 equiv per α -H atom) was added, and the deep purple solution that formed immediately was stirred for 1.5 h in the dark at room temperature. *p*-Chloranil (1.00 equiv per α -H atom)

was then added, and the reaction mixture was stirred for a further 1.5 h in the dark at room temperature. The deep brown solution was purified by flash chromatography on silica gel. The crude product was precipitated twice by adding a concentrated solution in dichloromethane to methanol to obtain the desired product.

GP2: General Procedure for the Stille Coupling Reactions. The terminal alkyne (1.00 equiv) was dissolved in dry Et₂O (10 mL per 1.00 mmol of alkyne) under a nitrogen atmosphere. The solution was cooled to -78 °C, and *n*-BuLi (1.6 M solution in hexanes, 1.13 equiv) was added via a syringe over a period of 5 min. The reaction mixture was stirred at -78 °C for 30 min and for a further 30 min at -30 °C and then was cooled to -78 °C again. Tri-*n*-butyltin chloride (1.15 equiv) was added dropwise via a syringe over a period of 5 min. The reaction mixture was stirred at -78 °C for 30 min and for a further 30 min at room temperature. The solution was hydrolyzed with water, the organic layer was separated and dried over MgSO₄, and the solvent was removed under reduced pressure. The residue was dried in vacuo for 3 h and then dissolved in dry THF (1 mL per 100 mg of liquid) under a nitrogen atmosphere. The aryl bromide **8** (1.00 equiv) was added, and the solution was degassed. Pd(PPh₃)₄ (0.05 equiv) was added, and the mixture was heated under reflux for 24 h under a nitrogen atmosphere. The solvent was removed in vacuo, the residue was dissolved in dichloromethane, and the organic layer was washed with water three times. After the organic layer was dried over MgSO₄, the solvent was removed under reduced pressure, and the crude product was purified by flash chromatography on silica gel. The crude product was precipitated twice by adding a concentrated solution in dichloromethane dropwise to methanol to obtain the desired tolan.

GP3: General Procedure for the Pd-Catalyzed Amination of Aryl Bromides and Aryl Iodides with Secondary Amines. The aryl bromide (aryl iodide) (1.10 equiv) and the secondary amine (1.00 equiv) were dissolved in absolute toluene (10 mL per 1.00 mmol of aryl bromide) under a nitrogen atmosphere. Pd₂(dba)₃·CHCl₃ (0.05 equiv), P(*t*-Bu)₃ (0.33 M in *n*-hexane, 0.04 equiv), and NaO-*t*Bu (2.50 equiv) were added, and the reaction mixture was stirred in the dark under a nitrogen atmosphere under reflux for 24 h. The solvent was removed in vacuo, and the residue was dissolved in dichloromethane. The organic layer was washed with water three times and dried over MgSO₄, and the solvent was removed under reduced pressure. Flash chromatography on silica gel afforded the desired product.

Synthesis of **8.** Sulfur monochloride (5.64 g, 41.8 mmol, 0.76 equiv) and dry aluminum chloride (2.87 g, 21.5 mmol, 0.39 equiv) were dissolved in freshly distilled sulfonyl chloride (700 mL), and the solution was stirred under reflux for 5 min. A solution of **9** (17.9 g, 55.0 mmol, 1.00 equiv) in sulfonyl chloride (500 mL) was added dropwise under heat while the initially yellow-orange solution turned to deep red. The reaction mixture was stirred for a further 8 h under reflux while the volume was kept constant by stepwise addition of sulfonyl chloride. The solution was cooled to room temperature, the solvent was removed

in vacuo, and ice water (600 mL) was added to the yellow-orange residue. NaHCO₃ was added until no gas evolution was recognized, and the mixture was heated under reflux for 1 h. The solution was cooled to room temperature, a concentrated HCl solution (14 M, 90 mL) was added, and the mixture was stirred under reflux for a further 1 h. The green crude product was filtered, washed with boiling *n*-hexane (3 × 50 mL), and dried in vacuo to afford 37.7 g (46.1 mmol, 84%) of a colorless solid: mp >300 °C; ¹H NMR (600 MHz, CDCl₃, 20 °C, TMS) δ = 6.98 (s, α-*H*, 1H); ¹³C NMR (151 MHz, CDCl₃, 20 °C, TMS) δ = 137.0 (quart.), 136.3 (quart.), 136.2 (quart.), 135.7 (quart.), 135.1 (2C, 2 × quart.), 134.8 (quart.), 134.7 (quart.), 134.1 (2C, 2 × quart.), 134.0 (quart.), 133.8 (quart.), 133.7 (quart.), 132.7 (quart.), 134.0 (2C, 2 × quart.), 132.5 (quart.), 125.6 (quart.), 56.8 (α-*C*); IR (KBr) $\tilde{\nu}$ = 2924 (w), 1521 (w), 1369 (m), 1336 (s), 1295 (s), 1238 (w), 1190 (w), 1116 (w), 809 (m), 784 (m), 712 (w), 691 (w), 674 (m), 639 (w), 609 (w), 522 (w), 419 (w) cm⁻¹; MS (FAB, 70 eV, 2-(octyloxy)-nitrobenzene) *m/z* (relative intensity) 1477 (27, M⁺), 1442 (8, M⁺ - Cl); APCI negative (high resolution) calcd for the X + 8 of [M - H]⁻ = C₁₉BrCl₁₄⁻, 804.47168, found 804.47097; Δ/ppm, 0.88.

Synthesis of Tolan 11. Compound **11** was synthesized from **10** (420 mg, 1.28 mmol) and **8** (1.03 g, 1.28 mmol) according to general procedure GP2. Flash chromatography on silica gel with 1:1 CH₂Cl₂/petroleum ether as eluent yielded 229 mg (218 μmol, 17%) of an intense yellow solid: *R_f* = 0.59 (CH₂Cl₂/petroleum ether = 1:1); mp 178 °C; ¹H NMR (600 MHz, acetone-*d*₆, 20 °C, TMS) δ = 7.43 (AA', 2H, NCCHCHCCC), 7.16 (AA', 4H, OCCHCH), 7.10 (s, 1H, α-*H*), 6.97 (BB', 4H, OCCHCHC), 6.80 (BB', 2H, NCCHCHCCC), 3.81 (s, 6H, OCH₃); ¹³C NMR (151 MHz, acetone-*d*₆, 20 °C, TMS) δ = 158.2 (2C, 2 × quart.), 151.6 (quart.), 140.2 (2C, 2 × quart.), 137.6 (quart.), 137.5 (quart.), 137.1 (quart.), 135.9 (quart.), 135.8 (quart.), 135.7 (quart.), 135.2 (quart.), 134.88 (quart.), 134.85 (quart.), 134.6 (quart.), 134.38 (quart.), 134.36 (2C, 2 × quart.), 134.3 (quart.), 134.2 (quart.), 133.9 (NCCHCHCCC), 133.24 (quart.), 133.21 (quart.), 128.8 (OCCHCH), 126.8 (quart.), 118.4 (NCCHCHCCC), 115.9 (OCCHCHC), 111.7 (quart.), 105.5 (quart.), 83.4 (quart.), 57.5 (α-*C*), 55.8 (OCH₃); IR (KBr) $\tilde{\nu}$ = 2927 (w), 2832 (w), 2198 (m), 1600 (w), 1542 (w), 1504 (vs), 1463 (w), 1440 (w), 1364 (w), 1338 (m), 1332 (m), 1292 (m), 1241 (s), 1174 (w), 1105 (w), 1037 (w), 827 (m), 809 (w), 709 (w), 686 (w), 577 (w), 534 (w) cm⁻¹; MS (EI, 70 eV) *m/z* (relative intensity) 1053 (100, M⁺), 1038 (8, M⁺ - CH₃); APCI positive (high resolution) calcd for [M + H]⁺ = C₄₁H₂₀Cl₁₄NO₂⁺, 1047.71279, found 1047.71219; Δ/ppm, 0.57. Elemental analysis calculated for C₄₁H₁₉Cl₁₄NO₂: C, 46.72; H, 1.82; N, 1.33. Found: C, 47.09; H, 2.16; N, 1.31.

Synthesis of Radical 2. Radical **2** was synthesized from **11** (100 mg, 94.4 μmol) according to general procedure GP1. Flash chromatography with 4:1 CH₂Cl₂/petroleum ether as eluent yielded 80.0 mg (76.0 μmol, 80%) of a red-brown solid: *R_f* = 0.84 (CH₂Cl₂/petroleum ether = 4:1); mp 185 °C (decomposition); IR (KBr) $\tilde{\nu}$ = 3026 (w), 2928 (w), 2833 (w), 2188 (s), 1685 (w), 1598 (m), 1505 (s), 1453 (w), 1336 (m), 1289 (w), 1241 (m), 1175 (w), 1106 (w), 1037 (w), 827 (w), 791 (w), 761 (w), 737 (w), 662 (w), 533 (w) cm⁻¹; MS (FAB, 70 eV, nitrobenzyl alcohol) *m/z* (relative intensity) 1052 (1, M⁺); APCI positive (high resolution) calcd for [M + H]⁺ = C₄₁H₁₉Cl₁₄NO₂⁺, 1046.70497, found 1046.70545; Δ/ppm, 0.46.

Synthesis of 12. Compound **12** was synthesized from **8** (1.00 g, 1.24 mmol) according to general procedure GP3. Flash chromatography with 1:1 CH₂Cl₂/petroleum ether as eluent afforded the crude product that was precipitated twice by adding a concentrated solution in acetone dropwise into methanol, to yield 155 mg (163 μmol, 13%) of a pale yellow solid: *R_f* = 0.60 (CH₂Cl₂/petroleum ether = 1:1); mp >290 °C; ¹H NMR (600 MHz, CD₂Cl₂, 20 °C, TMS) δ = 7.06 (s, 1H, α-*H*), 6.80–6.86 (8H, Aryl-*H*), 3.77 (2s, 6H, OCH₃); ¹³C NMR (151 MHz, CD₂Cl₂, 20 °C, TMS) δ = 155.8 + 155.7 (2 signals, NCCH or OCCH), 142.7 (quart.), 138.8 (2 signals, NCCH or OCCH), 136.97 (quart.), 136.95 (quart.), 136.8 (quart.), 136.0 (quart.), 135.9 (quart.), 135.7 (quart.), 135.5 (quart.), 135.4 (quart.), 134.9 (quart.), 134.41 (quart.),

134.40 (quart.), 134.0 (quart.), 133.94 (quart.), 133.93 (quart.), 133.86 (quart.), 132.90 (quart.), 132.85 (quart.), 122.4 + 122.2 (NCCHCHCO or NCCHCHCO), 114.89 + 114.86 (NCCHCHCO or NCCHCHCO) 56.9 (α-*C*), 55.8 (OCH₃); IR (KBr) $\tilde{\nu}$ = 3044 (w), 2931 (w), 2833 (w), 1505 (vs), 1463 (w), 1439 (w), 1404 (m), 1367 (w), 1341 (w), 1298 (m), 1243 (s), 1172 (w), 1111 (w), 1039 (m), 822 (m), 809 (m), 683 (w), 665 (w), 526 (w) cm⁻¹; MS (EI, 70 eV) *m/z* (relative intensity) 953 (100, M⁺), 938 (27, M⁺ - CH₃), 918 (44, 27, M⁺ - Cl); APCI positive (high resolution) calcd for C₃₃H₁₆Cl₁₄NO₂, 947.68149, found 947.68150; Δ/ppm, 0.01. Elemental analysis calculated for C₃₃H₁₅Cl₁₄NO₂: C, 41.56; H, 1.59; N, 1.47. Found: C, 41.88; H, 1.41; N, 1.47.

Synthesis of Radical 3. Radical **3** was synthesized from **12** (100 mg, 105 μmol) according to general procedure GP1. Flash chromatography with 4:1 CH₂Cl₂/petroleum ether as eluent yielded 70.0 mg (73.5 μmol, 70%) of a brown solid: *R_f* = 0.91 (CH₂Cl₂/petroleum ether = 4:1); mp 280 °C (decomposition); IR (KBr) $\tilde{\nu}$ = 3039 (vw), 2994 (w), 2932 (w), 2905 (w), 2833 (w), 1504 (vs), 1463 (w), 1439 (w), 1398 (w), 1335 (m), 1298 (w), 1244 (s), 1172 (m), 1110 (w), 1038 (m), 821 (m), 737 (w), 709 (w), 682 (vw), 665 (m), 586 (w), 526 (m) cm⁻¹; MS (EI, 70 eV) *m/z* (relative intensity) 952 (40, M⁺), 937 (6, M⁺ - CH₃), 902 (10, M⁺ - CH₃ - Cl), 882 (100, M⁺ - Cl₂); APCI positive (high resolution) calcd for [M + H]⁺ = C₃₃H₁₅Cl₁₄NO₂⁺, 946.67367, found 946.67184; Δ/ppm, 1.93.

Synthesis of 14. Pinacole borane **13** (400 mg, 927 μmol, 1.00 equiv) and the perchlorinated bromoaryl **8** (747 mg, 927 μmol, 1.00 equiv) were dissolved in dry toluene (10 mL) under a nitrogen atmosphere. Sodium carbonate (2.60 mL, 1.00 M in H₂O, 2.80 equiv) and Pd(PPh₃)₄ (21.4 mg, 927 μmol, 0.02 equiv) were added, and after degassing the solution was stirred under reflux and under an inert gas atmosphere for 24 h. The solvent was removed in vacuo, and the residue was dissolved in dichloromethane (100 mL). The organic layer was washed with water (2 × 100 mL) and dried over MgSO₄, and the solvent was removed under reduced pressure. The residue was purified by flash chromatography on silica gel (CH₂Cl₂/petroleum ether = 1:1). The crude product was precipitated twice by adding a concentrated solution of **14** in dichloromethane into methanol to obtain 300 mg (291 μmol, 31%) of a pale yellow solid: *R_f* = 0.57 (CH₂Cl₂/petroleum ether = 1:1); mp 198 °C; $\tilde{\nu}$ = 3034 (vw), 2999 (vw), 2945 (vw), 2928 (vw), 2900 (vw), 2831 (w), 1604 (m), 1504 (vs), 1463 (w), 1439 (w), 1392 (vw), 1361 (w), 1315 (m), 1294 (m), 1241 (s), 1178 (m), 1105 (w), 1080 (w), 1037 (m), 827 (m), 809 (m), 741 (w), 718 (w), 689 (w), 675 (m) cm⁻¹; ¹H NMR (600 MHz, acetone-*d*₆, 20 °C, TMS) δ = 7.16 (AA', 4H, NCCHCHCO), 7.13 (s, 1H, α-*H*), 7.09–7.14 (m, 2H, NCCHCHCC), 6.96 (BB', 4H, NCCHCHCO), 6.87–6.90 (m, 2H, NCCHCHCC), 3.81 (s, OCH₃); ¹³C NMR (151 MHz, acetone-*d*₆, 20 °C, TMS) δ = 157.7 (quart.), 150.1 (quart.), 143.3 (quart.), 140.8 (quart.), 137.7 (quart.), 137.6 (quart.), 137.2 (quart.), 135.85 (quart.), 135.84 (quart.), 135.4 (quart.), 135.1 (quart.), 134.84 (quart.), 134.79 (quart.), 134.3 (quart.), 134.24 (2 × quart.), 134.20 (2 × quart.), 134.18 (quart.), 133.13 (quart.), 133.11 (quart.), 130.5 (NCCHCHCC), 129.0 (quart.), 128.5 (NCCHCHCO), 118.5 (NCCHCHCC), 115.7 (NCCHCHCO), 57.5 (α-*C*), 55.7 (OCH₃); APCI positive (high resolution) calcd for [M + H]⁺ = C₃₉H₂₀Cl₁₄NO₂⁺, 1023.71279, found 1023.71143; Δ/ppm, 1.33.

Synthesis of Radical 4. Radical **4** was synthesized from **14** (200 mg, 194 μmol) according to general procedure GP1. Flash chromatography with 1:1 CH₂Cl₂/petroleum ether as eluent yielded 140 mg (136 μmol, 70%) of a red-brown solid: *R_f* = 0.94 (CH₂Cl₂/petroleum ether = 1:1); mp 240 °C (decomposition); IR (KBr) $\tilde{\nu}$ = 3039 (vw), 2994 (vw), 2950 (vw), 2932 (vw), 2905 (vw), 2834 (vw), 1603 (w), 1504 (s), 1464 (vw), 1437 (vw), 1320 (m), 1285 (w), 1242 (m), 1178 (w), 1103 (w), 1038 (m), 827 (m) cm⁻¹; APCI positive (high resolution) calcd for [M + H]⁺ = C₃₉H₁₉Cl₁₄NO₂⁺, 1022.70497, found 1022.70641; Δ/ppm, 1.41.

Synthesis of 16a. Compound **16a** was synthesized from **15a** (300 mg, 1.62 mmol) according to general procedure GP2. Flash chroma-

tography on silica gel with 1:1 CH₂Cl₂/petroleum ether as eluent yielded 222 mg (244 μmol, 15%) of a yellow solid: *R_f* = 0.52 (CH₂Cl₂/petroleum ether = 1:1); mp 175 °C; ¹H NMR (600 MHz, CD₂Cl₂, 20 °C, TMS) δ = 7.46 (AA', 2H, NCCHCHCCC), 7.01 (s, 1H, α-H), 6.88 (BB', 2H, NCCHCHCCC), 3.29 (t, ³J_{HH} = 5.4 Hz, 4H, NCH₂-CH₂), 1.68 (m, 4H, NCH₂CH₂CH₂), 1.63 (m, 2H, NCH₂CH₂CH₂); ¹³C NMR (151 MHz, CD₂Cl₂, 20 °C, TMS) δ = 152.8 (quart.), 136.93 (quart.), 136.92 (quart.), 136.2 (quart.), 135.5 (quart.), 135.4 (quart.), 135.3 (quart.), 134.6 (quart.), 134.4 (quart.), 134.3 (quart.), 134.2 (quart.), 134.0 (quart.), 133.93 (quart.), 133.92 (quart.), 133.90 (quart.), 133.8 (quart.), 133.7 (quart.), 133.6 (NCCHCHCCC), 132.9 (quart.), 132.8 (quart.), 126.5 (quart.), 114.9 (NCCHCHCCC), 112.1 (quart.), 109.9 (quart.), 56.9 (α-C), 49.2 (NCH₂CH₂), 25.8 (NCH₂CH₂CH₂), 24.7 (NCH₂CH₂CH₂); APCI positive (high resolution) calcd for the X + 6 of [M + H]⁺ = C₃₂H₁₆Cl₁₄N⁺, 909.68325, found 909.68318; Δ/ppm, 0.08.

Synthesis of 16b. Compound **16b** was synthesized from **15b** (300 mg, 1.60 mmol) according to general procedure GP2. Flash chromatography on silica gel with CH₂Cl₂ as eluent yielded 250 mg (274 μmol, 17%) of a yellow solid: *R_f* = 0.33 (CH₂Cl₂); mp 173 °C (decomposition); ¹H NMR (600 MHz, CD₂Cl₂, 20 °C, TMS) δ = 7.52 (AA', CCCHCH, 2H), 7.01 (s, α-H, 1H), 6.93 (BB', NCCHCH, 2H), 3.84 (m, OCH₂CH₂, 4H), 3.25 (m, NCH₂CH₂, 4H); ¹³C NMR (150 MHz, CD₂Cl₂, 20 °C, TMS) δ = 136.90 (quart.), 136.88 (quart.), 136.6 (quart.), 135.52 (quart.), 135.46 (quart.), 135.4 (quart.), 134.7 (quart.), 134.44 (quart.), 134.43 (quart.), 134.36 (quart.), 133.98 (quart.), 133.96 (quart.), 133.92 (quart.), 133.85 (quart.), 133.7 (quart.), 133.6 (CCCHCH), 133.5 (quart.), 133.4 (quart.), 132.9 (quart.), 132.8 (quart.), 126.3 (quart.), 114.9 (NCCHCH), 104.2 (quart.), 83.2 (quart.), 66.9 (OCH₂-CH₂), 56.9 (CICCCCH), 48.4 (NCH₂CH₂); IR (KBr) $\tilde{\nu}$ = 3080 (vw), 3044 (vw), 2959 (m), 2892 (vw), 2852 (w), 2202 (s), 1604 (vs), 1542 (m), 1514 (vs), 1448 (m), 1340 (vs), 1301 (s), 1261 (w), 1236 (vs), 1182 (m), 1124 (s), 1051 (w), 928 (s), 860 (w), 809 (s), 709 (m), 684 (m), 661 (w), 587 (w), 533 (m) cm⁻¹; MS (70 eV, EI) *m/z* (relative intensity) 911 (100, M⁺), 853 (19, M⁺ - C₃H₆O), 841 (6, M⁺ - Cl₂), 748 (31, M⁺ - C₃H₆Cl₃O); APCI positive (high resolution) calcd for [M + H]⁺ = C₃₁H₁₂Cl₁₄NO⁺, 903.65528, found 903.65435; Δ/ppm, 1.03.

Synthesis of Radical 5. Radical **5** was synthesized from **16a** (123 mg, 135 μmol) according to general procedure GP1. Flash chromatography on silica gel with 1:1 CH₂Cl₂/petroleum ether as eluent yielded 75 mg (82.5 μmol, 61%) of a red-brown solid: *R_f* = 0.55 (CH₂Cl₂/petroleum ether = 1:1); mp 172–178 °C (decomposition); IR (KBr) $\tilde{\nu}$ = 2933 (m), 2852 (w), 2186 (s), 1601 (s), 1522 (s), 1464 (w), 1451 (w), 1384 (m), 1337 (s), 1320 (m), 1259 (w), 1233 (s), 1187 (m), 1126 (m), 1023 (m), 937 (w), 918 (w), 863 (w), 817 (m), 737 (w), 711 (m), 661 (w), 532 (w) cm⁻¹; APCI positive (high resolution) calculated for [M + H]⁺ = C₃₂H₁₅Cl₁₄N⁺, 902.68348, found 902.68346; Δ/ppm, 0.41.

Synthesis of Radical 6. Starting from tolane **16b** (100 mg, 110 μmol, 1.00 equiv), compound **6** was prepared according to general procedure GP1. Flash chromatography on silica gel with CH₂Cl₂ as eluent yielded

80.1 mg (87.9 μmol, 80%) of a dark brown solid: *R_f* = 0.42 (CH₂-Cl₂); mp 180 °C (decomposition); IR (KBr) $\tilde{\nu}$ = 3093 (vw), 3048 (vw), 2933 (m), 2851 (w), 2185 (vs), 1602 (vs), 1522 (vs), 1450 (w), 1384 (m), 1337 (vs), 1233 (s), 1186 (m), 1126 (m), 1022 (m), 937 (w), 918 (vw), 863 (w), 817 (m), 737 (w), 711 (m), 661 (w), 533 (w) cm⁻¹; MS (70 eV, FAB, 2-(octyloxy)nitrobenzene) *m/z* (relative intensity) 910 (<1, M⁺), 840 (<1, M⁺ - Cl₂); APCI positive (high resolution) calculated for [M + H]⁺ = C₃₁H₁₅Cl₁₄NO⁺, 904.66262, found 904.66345; Δ/ppm, 0.38.

Synthesis of Compound 18. Compound **18** was synthesized starting from **17**¹⁰⁵ (1.00 g, 6.90 mmol) and **8** (5.56 g, 6.90 mmol) according to general procedure GP2. Flash chromatography with petroleum ether as eluent afforded 660 mg (759 μmol, 11%) of an intense yellow solid: *R_f* = 0.28 (petroleum ether); mp 183 °C; ¹H NMR (600 MHz, CD₂Cl₂, 20 °C, TMS) δ = 7.46 (AA', NCCHCH, 2H), 7.01 (s, α-H, 1H), 6.69 (BB', NCCHCH, 2H), 3.02 (s, N(CH₃)₂, 6H), ¹³C NMR (150 MHz, CD₂Cl₂, 20 °C, TMS) δ = 151.6 (quart.), 137.0 (quart.), 136.0 (quart.), 135.5 (quart.), 135.4 (quart.), 135.1 (quart.), 134.6 (quart.), 134.4 (quart.), 134.3 (quart.), 133.90 (quart.), 133.88 (quart.), 133.6 (NCCHCH), 132.9 (quart.), 132.8 (quart.), 132.0 (quart.), 131.9 (quart.), 126.6 (quart.), 125.4 (quart.), 112.0 (NCCHCH), 107.9 (quart.), 105.6 (quart.), 105.0 (quart.), 83.0 (quart.), 82.5 (quart.), 56.9 (α-C), 40.2 (N(CH₃)₃); IR (KBr) $\tilde{\nu}$ = 3093 (vw), 3039 (vw), 2896 (w), 2860 (w), 2806 (w), 2197 (s), 1605 (vs), 1542 (s), 1521 (s), 1482 (vw), 1444 (m), 1362 (s), 1345 (s), 1298 (w), 1234 (w), 1168 (m), 1118 (w), 1064 (w), 946 (w), 860 (w), 813 (s), 709 (m), 530 (m) cm⁻¹; APCI positive (high resolution) calcd for X + 6 of [M + H]⁺ = C₂₉H₁₂-Cl₁₄N⁺, 869.65187, found 869.65167; Δ/ppm, 0.23.

Synthesis of Radical 7. Radical **7** was synthesized starting from **18** (150 mg, 172 μmol) according to general procedure GP1. Flash chromatography with CH₂Cl₂ as eluent yielded 104 mg, (120 μmol, 70%) of a red-brown solid: *R_f* = 0.96 (CH₂Cl₂); mp 190 °C (decomposition); IR (KBr) $\tilde{\nu}$ = 3093 (vw), 3039 (vw), 2918 (w), 2855 (w), 2806 (w), 2183 (s), 1604 (vs), 1526 (s), 1443 (m), 1362 (s), 1338 (s), 1258 (w), 1237 (m), 1179 (m), 1139 (vw), 1064 (w), 946 (m), 815 (s), 737 (w), 711 (m), 655 (w), 530 (w) cm⁻¹; APCI positive (high resolution) calcd for X + 6 of [M + H]⁺ = C₂₉H₁₁Cl₁₄N⁺, 868.64404, found 868.64287; Δ/ppm, 1.35.

Acknowledgment. We are grateful to the Deutsche Forschungsgemeinschaft for financial support, to Heraeus GmbH for chemicals and to Dr. Büchner for obtaining the mass spectra, and to Christian Müller and André Schuster for synthetic work.

Supporting Information Available: Appendix, with comments about the use of the polarity function and derivation of eq 7. This material is available free of charge via the Internet at <http://pubs.acs.org>.

JA068235J

(105) Miki, Y.; Momotake, A.; Arai, T. *Org. Biomol. Chem.* **2003**, *1*, 2655–2660.